JULY 2019

M.Sc.in Physics Engineering

EDA BAY USLU

REPUBLIC OF TURKEY

GAZİANTEP UNIVERSITY

GRADUATE SCHOOL OF NATURAL & APPLIED SCIENCES

INVESTIGATION OF THE EFFECTS OF BETA RAYS ON PHOSPHORESCENT MATERIALS

M.Sc. THESIS

IN

PHYSICS ENGINEERING

BY

EDA BAY USLU

JULY 2019

INVESTIGATION OF THE EFFECTS OF BETA RAYS ON PHOSPHORESCENT MATERIALS

M.Sc. Thesis

in

Physics Engineering

Gaziantep University

Supervisior

Prof. Dr. Hayriye Tütüncüler

by

Eda BAY USLU

July 2019

REPUBLIC OF TURKEY

GAZİANTEP UNIVERSITY

GRADUATE SCHOOL OF NATURAL & APPLIED SCIENCES

PHYSICS ENGINEERING

Name of the thesis: Investigation of the Effects of Beta Rays on Phosphorescent Materials

Name of the student: Eda BAY USLU

Exam date: 11.07.2019

Approval of the Graduate School of Natural and Applied Sciences

Prof. Dr. A. Necmeddin YAZICI

Director

I certify that this thesis satisfies all the requirements as a thesis for the degree of Master of Science.

Prof. Dr. Ramazan KOÇ

Head of Department

This is to certify that we have read this thesis and that in our opinion it is fully adequate, in scope and quality, as a thesis for the degree of Master of Science.

Prof. Dr. Hayriye TÜTÜNCÜLER

Supervisor

Examining Committee Members:	Signature
Prof. Dr. Eser OLĞAR	……
Prof. Dr. Hayriye TÜTÜNCÜLER	……
Assist. Prof. Dr. Tuba DENKÇEKEN	……

I hereby declare that all information in this document has been obtained and presented in accordance with academic rules and ethical conduct. I also declare that, as required by these rules and conduct, I have fully cited and referenced all material and results that are not original to this work.

Eda BAY USLU

ABSTRACT

INVESTIGATION OF THE EFFECTS OF BETA RAYS ON PHOSPHORESCENT MATERIALS

BAY USLU, Eda
M.Sc. Thesis in Physics Engineering
Supervisor: Prof. Dr. Hayriye TÜTÜNCÜLER
July 2019
52 pages

The aim of this thesis is to investigate the effects of beta radiation on phosphorescent materials. Nowadays phosphorescent materials are used to get the production of more efficient beta voltaic nuclear batteries. They convert the kinetic energy of particles to fluorescence by using phosphor material and then to convert electricity via photovoltaic cell. We have researched the effects of beta particles by analyzing the parameters such as range and generation rate for different type of phosphorescent materials that are used in nuclear batteries. These parameters effectively improve the output performance and energy conversion efficiency in nuclear batteries.

Key words: Phosphorescent Materials, Beta rays, Stopping Power, Range, Absorption Coefficient, Reflection Coefficient, Generation Rate.

ÖZET

FOSFOR MATERYALLER ÜZERİNDE BETA IŞINLARININ ETKİSİNİN ARAŞTIRILMASI

BAY USLU, Eda
Yüksek Lisans Tezi, Fizik Mühendisliği
Danışman: Prof. Dr. Hayriye TÜTÜNCÜLER
Temmuz 2019
52 sayfa

Bu tezin amacı beta radyasyonun fosforlu materyaller üzerindeki etkilerini araştırmaktadır. Günümüzde fosforlu malzemeler, daha verimli beta voltaik nükleer pillerin üretiminde kullanılmaktadır. Parçacıklar kinetik enerjisini fosfor materyali kullanarak flüoresansa dönüştürürler ve daha sonra fotovoltaik hücre yoluyla elektriğe dönüştürürler. Nükleer bataryalarda kullanılan farklı tip fosforlu malzemelerin menzil ve üretim hızı gibi parametreleri analiz ederek beta parçacıklarının etkilerini araştırdık. Bu parametreler nükleer pillerde çıkış performansını ve enerji dönüşüm verimliliğini etkin bir şekilde geliştirir.

Anahtar Kelimeler: Fosfor Materyaller, Beta Işınları, Durdurma Gücü, Menzil, Absorpsiyon Katsayısı, Yansıma Katsayısı, Üretim Hızı.

“Dedicated to my family and my husband”

ACKNOWLEDGEMENTS

I express sincere appreciation to my supervisior Prof. Dr. Hayriye Tütüncüler for her continues support, guidance and encouragement. Also, my great thanks go to her for her advice, suggestion and motherly expression.

I would like to thank to my family for their patience and support and especially my husband Salih USLU and my little brother Berkay BAY. Their continuos encouragement and advice have helped me to complete this thesis.

TABLE OF CONTENTS

Page

LIST OF TABLES

Page

LIST OF FIGURES

Page

LIST OF SYMBOLS

B	Binding energy of an electron orbit
T_+	The kinetic energies of the positron
T_-	The kinetic energies of the electron
r_e	Classical electron radius
m_0c^2	Electron rest energy
u	Atomic mass unit
δ	Density effect correction
Z	Atomic number
ρ	Density
A	Atomic weight
I	The mean ionization (excitation) energy
τ	The ratio of the electron relativistic energy to its rest energy
β_h	Correction factor for heavy charged particles
β_e	Correction factor for electrons
S	Stopping power
$\frac{S}{\rho}$	Mass stopping power
R	Range
E_{max}	The maximum kinetic energy
E_{mean}	The mean kinetic energy
g(R)	Generation rate
ε	Average energy

α	Absorption coefficient
Φ	The incident beta flux
r	The reflection coefficient
E_g	Bandgap energy
μ_m	The mass attenuation coefficient
T_h	The kinetic energy for heavy charged particles

LIST OF ABBREVIATIONS

MEMS	Microelectromechanical systems
RL	Radioluminescent
CSDA	Continuous slowing down approximation
ISC	Inter system crossing
PV	Photovoltaic

CHAPTER 1

INTRODUCTION

Luminescent materials, known as phosphorus, have a long tradition in some areas. These areas are especially lighting, display and imaging techniques. At present, materials that provide bright light have significant advantages. It provides superior quality emission spectrum for white LEDs. It provides clear computerized radiography images at low irradiation dose. It empowers our light-based communication with rare earth doped (fiber) lasers. A specific type of luminescence is permanent luminescence, also denoted as “glow in-the-dark”, where the emission can continue for hours after the excitation ends.

Recently, Zn and Sr based phosphor compounds have great attention in the design of nuclear battery [1]. Especially, zinc oxide (ZnO), zinc sulfide (ZnS) and strontium aluminate phosphors operated by Eu^{2+}, Dy^{3+} ions have attracted a lot of caution since they show very good properties such as high quantum efficiency, long persistence of phosphorescence and high stability. Nuclear batteries that convert radioactive decay energy into electrical energy are a potential applicant as energy provider for microelectromechanical systems (MEMS). Many species found in nuclear batteries have focused more on betavoltaic micro batteries and have tried to increase its efficiency in recent years. However, structural damage of the remaining semiconductor material exposed to abnormally high energy radioactive radiation reduces the efficiency of the battery and its life. Low radiation stability of these converters minimizes the conversion efficiency over time. To address this delimitation, the radioluminescent (RL)nuclear battery is an amazing select. The phosphor layer in the RL nuclear battery absorbs the beta rays. The radiation energy is transformed into luminescence energy, which is then transformed into electricity.

To improve the efficiency of RL nuclear battery thickness of phosphor layer is also important. This thickness is obtained from the range of charged particle in the phosphor material. The energy loss of charged particles per length in material is important in the fields of radiation physics and radiation dosimetry. This quantity, is called the stopping power of the medium for the particle and is related with the range which charged particles propagate until stop. To determine the range of charged particles, energy loss mechanism should be analysed very well. The number of electron and hole pairs generated in such phosphors, generation rate, are also important in RL nuclear battery. This study covers the theoretical investigation of these parameters.

Radioluminescence nuclear batteries have undergone great development in recent years. For examples, to analyse the effect of phosphor layer parameters on the battery, the electrical properties are measured, phosphorus based nuclear batteries are designed [2], and the electron stopping power of some elements is calculated [3]. Stable and efficient power systems with a long life time have tremendous potential applications in many fields, including ultra-low power devices, autonomous systems, and aerospace electronics. In particular, the power sources can be used in places where their maintenance and replacement is extremely difficult or even impossible. Prime candidates for such power systems are radioisotope-motivated generators.

Batteries, such as fuel and solar cells, they cannot provide the optimal powers which have large volumes, short lifetime and low-level environmental adaptations are giving this trouble [2]. A nuclear battery can convert nuclear power into usable electrical power for years, or even decades (depending on the radioactive isotope used). Other advantages of radioisotope power sources include small size, low weight, high adaptability, stable power output, and high reliability [4,5].

When beta radioluminescence nuclear battery's parameter is optimized, it gives 25% efficiency in theorically [2]. Increasing thickness of phosphor provides keeping more energy by beta particles in the phosphor layer. To give examples for using area of this material (phosphor) are Laptop computer's batteries can stand at least 5 years without any charge and if it is used satellite at space, there is no necessary to repairing or other controlling [2].

In literature, the effect of x-rays on radioluminescence nuclear cells has been investigated. According to the results obtained, X-rays are more safe than gamma rays but when they are exposed to X-rays for a long time, radiation damage has occurred [6]. When the phosphorus layer was used, it was investigated that this damage was effectively reduced. Beta-isotope batteries can provide power without requiring less volume coverage and maintenance [7]. The radioactive sources of low-energy beta particles are preferred because they cause radiation damage to the energy conversion materials of high energy particles (147Pm, 63Ni, 90Sr) [8]. These batteries have a long service life, strong adaptation, high stability; they did not need energy charge during service and most importantly they could be miniaturized [2,8]. Intensive energy sources are important in the development of terrestrial and space applications and remote sensors. Nuclear batteries using beta-emitting radioisotopes were found to have a thousand-fold more energy density than chemical batteries [9]. The performance of the nuclear batteries depends on the radiation carrying properties of radioisotopes and the energy transformations [10].

The design of nuclear batteries for indirect energy conservation has two important points. Firstly, high radioluminescence protection and high tolerance for ionizing radiation. Secondly, Proper matching of the emission wavelength with the spectral reaction of the photovoltaic (PV) device. The use of beta radioluminescence nuclear batteries is still limited in areas where total energy conversion capacity is present. The phosphorus layers are important for beta radioluminescence nuclear batteries with a new indirect transformation process. They have an important role in the protection of semiconductor materials, absorption of incident radiation and the transport of emitted light. Transmission is a very good way to increase the power of the batteries. Investigation of an appropriate phosphorus layer structure can improve to increase the performance of beta radioluminescence nuclear batteries.

In chapter 1, general information about radioluminescence nuclear batteries is given. The advantages and applications of nuclear batteries are mentioned. In addition, previous researches on this subject are mentioned. In chapter 2, interaction of electrons with matter and scattering resulting from this interaction is mentioned. In chapter 3, general information about phosphors materials is given. The mechanisms of phosphors and their application areas are mentioned. In chapter 4, the theoretical calculations and results of our study are mentioned. In chapter 5, the general results of our study are discussed.

CHAPTER 2
RADIATION PHYSICS

Materials can be processed with radiation to change their physical, chemical and biological properties. With this process, the properties of the new materials can be changed as desired. Radiation physics knowledge is required in many areas. These areas are the nature of electromagnetic radiation, the interaction of matter with radiation, the structure of matter and the fields of nuclear physics [11].

2.1 Basic Forces in Nature

Some interactions between the various particles were observed. These interactions are strong and weak nuclear forces, electromagnetic forces, and gravitational forces. Some of these forces have unlimited ranges, while others have very short ranges. Each of the forces are caused by some important properties of the particles.

2.1.1 The Electromagnetic Force

The electromagnetic force is the force acting between two objects with an electric charge. This force is very strong and long range. It can be observed in different forms. These are the interaction between electrons and nuclei and the basic interaction between atoms in molecules and solids.

The electrical force is an aspect of the electromagnetic force. It is an attractive or repulsive force relating with the characteristics of the charges. Two positive or negative charges repel each other. But the opposite charges attract each other.

The magnetic force is an aspect of the electromagnetic force. This force depends on the interaction of the magnetic field between two charged objects. Two magnetic north poles or two magnetic south poles repel each other. A magnetic north pole and a magnetic south pole attract each other.

2.1.2 The Strong Nuclear Force

A strong nuclear force is a very powerful force that holds protons and neutrons together in the atom. They have very short distance about 10^{-15} m [12]. It is the most powerful of the basic forces. This force connects the quarks. Thus protons, neutrons and many subatomic particles can be formed.

Quarks are basic particles containing protons and neutrons. As a result of strong forces, it is always connected to other quarks. A proton consists of two “up” quarks and a “down” quark, while a neutron consists of two “down” quarks and an “up” quark.

The strong nuclear force tries to keep the nucleus together. But electric forces try to break the nucleus. Therefore, the electric force can break the nucleus in large atoms. As a result of that it results alpha decay.

2.1.3 The Weak Nuclear Force

The weak nuclear force is effective in quarks that form protons and neutrons. It is a very short-range forces about 10^{-18} m. It is much weaker than electricity and strong forces. It acts over extremely small distances and causes beta decay. The sun would not shine if there was no weak nuclear force. Because it causes the protons to turn into neutrons. Thus, nuclear fusion occurs.

2.1.4 The Gravitational Force

The gravitational force occurs between two objects with mass. This force has a very weak, attractive, long range and unlimited range. It is the weakest of the fundamental forces.

2.2 Basic Particles

The basic particles are separated in two basic classes. These are quarks and leptons. Quarks show strong interactions. It is a component of hadrons with fractional electric charges. The hadrons are protons and neutrons. There are various quarks known as up, down, strange, charm, top and bottom. Leptons are weakly interacting particles. These particles are composed of electrons, muons, taus and neutrinos of these particles.

Table 2.1 Four fundamental interactions

INTERACTION	RELATIVE STRENGTH	RANGE (m)	PARTICLE(S) AFFECTED	EXCHANGE PARTICLES
Strong	1	10^{-15}	quarks	gluons
Electromagnetic	10^{-2}	∞	electrically charged	photon
Weak	10^{-6}	10^{-18}	quarks and leptons	boson
Gravitational	10^{-43}	∞	all	graviton

2.3 Classification of Radiation

Radiation is the energy form of the wave or particles. There are many radiations around us. When radiation is mentioned, the first thing that comes to mind is atomic energy, radioactivity and nuclear power. However, there are many different types of radiation. Sound and visible light are also radiation types. Other types of radiation are ultraviolet radiation, infrared radiation, and radio and television signals. There are various types of radiation in the electromagnetic spectrum.

In other words, radiation is the transfer of energy from one place to another. Radiation is divided into two main categories. These are ionizing and non-ionizing radiation and shown in Figure 2.1.

Non-ionizing radiation is the radiation that cannot ionize the substance. Examples of this radiation are visible light, signals from mobile phones and radio waves, baby monitors, cordless phones, and garage-door openers.

The radiation that ionizes the substance directly or indirectly is called ionizing radiation. This radiation is caused by both natural and man-made radioactive materials. Examples of ionizing radiation are radiation emission from uranium and high frequency waves (in electromagnetic spectrum). Ionizing radiation consists of two parts as direct and indirect ionizing radiation [13].

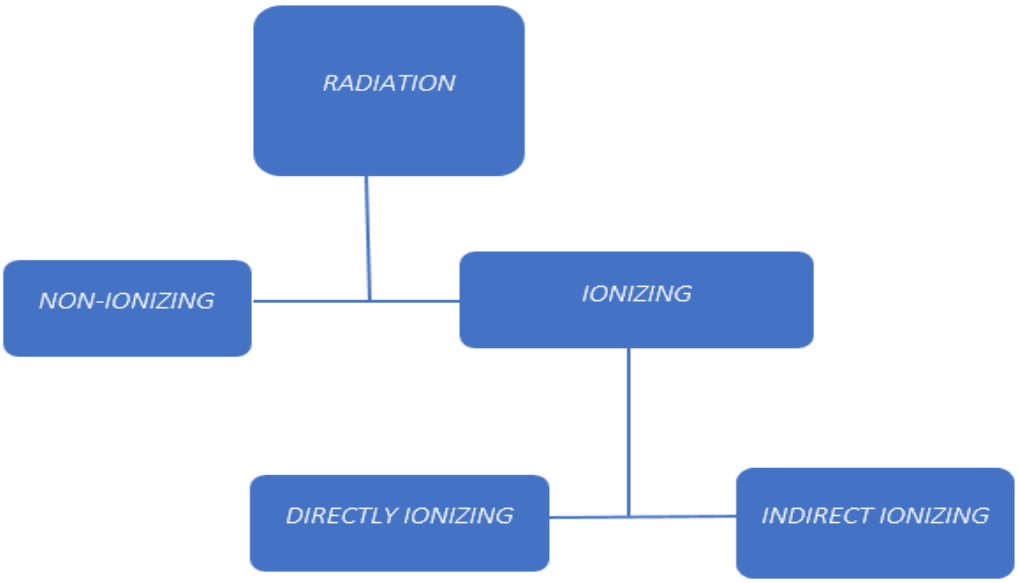

Figure 2.1 Classification of radiation

Directly ionizing radiation is the accumulation of energy as a result of Coulomb interaction with ionizing charged particle and an electron in orbit of the atom in the medium. Directly ionizing radiation is caused by charged particles. These are electrons, protons, particles and heavy ions.

Indirectly ionizing radiation is caused by photons or neutrons. Photons are free electrons or positrons, and neutrons are free protons or heavier ions. The indirectly ionizing radiation is carried out by a two-step process [14]. Firstly, the rapidly charged particle is released into the medium. Secondly, the released charged particles deposit energy to the medium through direct Coulomb interactions with orbital electrons of the atoms in the medium.

Ionizing photon radiation can be classified in four ways. These are characteristic X-rays, bremsstrahlung, gamma rays and annihilation quanta.

- Characteristic X rays are caused by electron transitions between atomic shells.
- Bremsstrahlung is caused by electron–nucleus Coulomb interactions.
- Gamma rays are caused by nuclear transitions.
- Annihilation radiations are caused by positron–electron annihilation.

Ionizing radiation is available in two ways: natural and man-made (artificial). Natural radiation is found in many forms around us. Our world has a significant amount of ionizing radiation and our body has adapted to this situation. During the formation of the solar system and the interaction of cosmic rays with the molecules in the atmosphere, many radioisotopes are formed. Continuous ionizing radiation is present in the natural environment. This radiation is called background radiation.

The United Nations Scientific Committee on the Effects of Atomic Radiation (UNSCEAR) identifies four major sources of public exposure to natural radiation. These are cosmic radiation, terrestrial radiation, inhalation, and ingestion. Radioisotopes can be produced by the operation of nuclear reactors and by radioisotope generators. There are many man-made radioisotopes. The produced radioisotopes are used in nuclear medicine, biochemistry, agriculture and manufacturing industry.

In addition, there are several types of ionized radiation. Some of these are alpha, beta and gamma radiation.

2.3.1 Alfa decay

Alpha decay emits alpha particles as a result of nuclear fragmentation. Alpha decay can be shown as follows [15].

$$^{238}_{92}U \rightarrow {}^{4}_{2}He + {}^{234}_{90}Th \quad (2.1)$$

As a result of this nuclear fragmentation, the uranium atom was transformed into a thorium atom. Then the alpha particle has emitted. The result of alpha decay consists of a core, two protons and two neutrons. This causes a smaller nucleus, which is more stable. Since the helium atom has two protons and two neutrons, the emitted particle is actually a helium atom.

Consequently, alpha radiation consists of alpha particles. These particles carry a double positive charge. Due to their large masses and charges, they can penetrate very little into the materials. Alpha radiation can be stopped with a piece of paper. Therefore, they do not create a radiation hazard.

2.3.2 Beta Decay

The beta particle is a high-energy electrode released from the nucleus. Furthermore, beta decay can be considered as a breakdown of a neutron to an electron and an electron. As a result of decay, the proton remains in the nucleus and increases the number of atoms by +1. The electron is removed from the nucleus and emits beta radiation. Thorium-234 is a nucleus that undergoes beta decay. Here is the nuclear equation for this beta decay [15].

$$^{234}_{90}\mathrm{Th} \rightarrow {}^{0}_{-1}\mathrm{e} + {}^{234}_{91}\mathrm{Pa} \tag{2.2}$$

As a result, beta radiation emerges from the nucleus of an atom. They are composed of charged particles that are physically identical to electrons. These particles have a negative charge. Because they are very small, they can diffuse deeper. They're stronger than alpha particles. Plastic, glass or metal sheets can be used to stop beta radiation.

2.3.3 Gamma Decay

Frequently, gamma ray production accompanies nuclear reactions of all types. In the alpha decay of U-238, two gamma rays of different energies are emitted in addition to the alpha particle [15].

$$^{238}_{92}\mathrm{U} \rightarrow {}^{4}_{2}\mathrm{He} + {}^{234}_{90}\mathrm{Th} + 2{}^{0}_{0}\gamma \tag{2.3}$$

Gamma radiation includes photons originating from the nucleus. This radiation is electromagnetic radiation. They do not have weight because they are composed of photons. Therefore, they can penetrate deeply and are dangerous.

Table 2.2 Properties of particles

Particle	**Mass**	**Penetrating Power**	**Ionizing Power**	**Shielding**
Alpha	4 atomic mass unit (amu)	Very Low	Very High	Paper Skin
Beta	1/2000 atomic mass unit	Intermediate	Intermediate	Aluminum
Gamma	0 (energy only)	Very High	Very Low	2 inches lead

Table 2.3 Nuclear Decays

Decay type	**Radiation Emitted**	**Generic Equation**
Alpha Decay	${}^{4}_{2}\alpha$	${}^{A}_{Z}X \rightarrow {}^{A-4}_{Z-2}X' + {}^{4}_{2}\alpha$
Beta Decay	${}^{0}_{-1}\beta$	${}^{A}_{Z}X \rightarrow {}^{A}_{Z+1}X' + {}^{0}_{-1}\beta$
Gamma Decay	${}^{0}_{0}\gamma$	${}^{A}_{Z}X'' \xrightarrow{Relaxation} {}^{A}_{Z}X' + {}^{0}_{0}\gamma$

2.4 Interaction of Photons with Matter

When energy particles move, they lose energy in matter. This causes electrical interactions to energy loss. But photons lose energy in a different way. Because they have a charge neutrality. Therefore, photons can move to a certain distance without interacting with the atom. This distance is related on the energy of the photon. It is statistically obtained by the probability of interaction per unit length.

The photons are sometimes absorbed, sometimes lost and sometimes scattered. There may or may not be energy loss during interactions. For example, there is no energy loss in Thomson scattering and Rayleigh scattering, but there is energy loss in photoelectric absorption, Compton scattering, photonuclear reaction and pair creation.

2.4.1 Thomson Scattering

The free electron is oscillated in response to the electrical vector of the electromagnetic wave. These scattering is important for low energies. Oscillating electron emits radiation. This radiation has the same frequency as the incoming wave. There is no energy loss, only the angle of deflection is changed.

2.4.2 Photoelectric Effect

Photoelectric effect is the photon rupture of light from matter. The broken electrons are called photoelectron. The energy of photoelectrons is inversely proportional to the wavelength of the radiation. The energy of the incoming radiation has the energy of a photon.

The energy of the photon is E=hv, where h is Planck's constant and v is the frequency. When an electron in the substance completely absorbs the photon, the photoelectron is produced. Thus, the incoming photon disappears. The kinetic energy of a photo electron, T, is represented by [12]

$$T = hv - B \tag{2.4}$$

where B is the binding energy of an electron orbit.

2.4.3 Compton Scattering

Compton scattering is the scattering when high-energy photons interact with the atom. The energy of the photons after scattering is reduced. This is a non-elastic scattering. This indicates that the light is not just a wave. The light should behave like particles to describe the scattering of the compton. Compton's experiment confirmed that energy is directly proportional to frequency and acts as a particle.

2.4.4 Pair Creation

When photon energy is at least twice the electron rest mass, the photon is converted to a pair of electron-positron in the vicinity of a nucleus. If the energy of the photon is greater than four times the electron rest mass energy in pair creation, it occurs in the atomic electron field. But this possibility is very low. This process is called triplet pair creation. Therefore, the photon energy hv is converted to [12]

$$h\nu = 2mc^2 + T_- + T_+ \quad (2.5)$$

where T_+ and T_- represent the kinetic energies of the positron and electron, respectively. The energy distribution of the electron and positron continuously varies in the range between 0 and ($h\nu - 2mc^2$). Those energy spectra are almost the same. The threshold energy is 1.022 MeV.

2.4.5 Photonuclear Reaction

The photonuclear reaction is the removal of nucleons from the nucleus absorbent photons. For this to occur, the photons must be larger than the binding energy of the nucleons. The possibility of a photonuclear event is very low. Since it also produces neutrons, it is important to be protected from radiation. After this reaction, the nucleus becomes radioactive. These reasons from this reaction play a significant role in the vicinity of high-energy electron accelerators.

2.5 Interaction of Heavy Charged Particles with Matter

When the charge particles propagates through matter, their energies are lost by ionization and excitation of atoms or molecules in the medium. The mean energy loss of charged particles per unit length is important in radiation physics. This quantity is known as stopping power of the material for the particle. The stopping power for heavy charged particles has two parts, the collisional (electronic) stopping power due to interaction with electrons of the material and nuclear stopping power.

2.5.1 Collision Stopping Power

The collision stopping power formula for heavy charged particles was derived by H.A. Bethe using relativistic quantum mechanics [16-19].

$$S_{col} = -\frac{dE}{dx} = \frac{4\pi r_e^2 m_0 c^2 z^2 \rho Z N_A}{\beta_h^2 A} \ln \frac{2m_0 c^2 \beta_h^2}{I(1-\beta_h^2)} - \beta_h^2 \quad (2.6)$$

r_e=2.817 940 289 4e10^{-15} m is the classical electron radius, m_0c^2=0.510 998 910 MeV is the electron rest energy, z = charge of heavy charged particle, A = atomic mass of the target atom, ρ is the density of phosphor materials, N_A = Avogadro constant, and β_h is a correction factor for heavy charged particles. This is represented, if the mass of particle, M, and the kinetic energy for heavy charged particles, T_h, are used, as [16]

$$\beta_h = \sqrt{1 - \left(\frac{Mc^2}{T_h + Mc^2}\right)^2} \tag{2.7}$$

The other terms in eqn (2.6) are parameters describing the material of interest: Z is the atomic number, and ρ is the density.

2.5.2 Nuclear Stopping Power

Due to the elastic scattering of heavy charged particles, energy loss occurs. The energies of these particles are less than 10 keV. This is called nuclear stopping power. Putting the differential cross section for elastic scattering as $d\sigma_{el}/d\Omega$, the nuclear stopping power S_{nuc} is represented by [16]

$$S_{nuc} = \frac{2\pi\rho N_A}{A} \int_0^{\pi} \frac{d\sigma_{el} W(\theta, T_h) \sin\theta d\theta}{d\Omega} \tag{2.8}$$

where $W(\theta,T_h)$ is the recoil energy, which depends on the scattering angle, θ. Using the mass of the particle, M, and the mass of the target atom, M_T, $W(\theta,T_h)$ is given by [16]

$$W(\theta, T_h) = 4T_h \frac{M_T M}{(M_T + M)^2} \sin^2\frac{\theta}{2} \tag{2.9}$$

The elastic scattering cross section for a high-energy region above a few MeV is described by the Rutherford cross section:

$$\frac{d\sigma_{el}}{d\Omega} = \frac{N_A Z^2 z^2 r_e^2}{4A} \frac{m_0 c^2}{p\beta_h} \frac{1}{\sin^4\frac{\theta}{2}} \tag{2.10}$$

in which the momentum of the heavy charged particle, p, is given by [16]

$$p = \frac{1}{c}\sqrt{(E + Mc^2)^2 - (Mc^2)^2} \tag{2.11}$$

Since the radiative stopping power can be neglected for heavy charged particles, the total stopping power is the sum of collision loss and nuclear loss.

$$S_{tot} = S_{col} + S_{nuc} \tag{2.12}$$

The contribution of nuclear stopping power to the total stopping power is negligible for the energy region greater than 10 keV; however, it increases as the energy is lowered. That amounts to about 30% at 1 keV.

2.5.3 Ranges

The distance that the charged particles advance until stop is called the range. It is assumed that charged particles continously slow down until the initial energy is completely lost. For heavy charged particles, the effect of multiple scattering is not considered. It is approximated those continuously slow down nearly on a straight line. From the continuous slowing down (CSDA) approximation, range $R(T_h)$ is obtained by [12]

$$R(T_h) = \int_0^{T_h} [S_{col}(T_h) + S_{nuc}(T_h)]^{-1} dT_h \tag{2.13}$$

A relationship between the ranges of different types of two particles with the same initial velocity is represented by [12]

$$\frac{R_1(\beta_h)}{R_2(\beta_h)} = \frac{z_2^2 M_1}{z_1^2 M_2} \tag{2.14}$$

where z_1 and z_2 are charges, M_1 and M_2 are rest masses. Assuming the range of the proton as particle 2 is known, the range R of the other particle becomes [12]

$$R(\beta_h) = \frac{M}{z^2} R_p(\beta_h) \tag{2.15}$$

where $R_p(\beta_h)$ is the proton range.

2.6 Interaction of Electrons with Matter

When the electron with the energy passes through the substance, it interacts with the atomic nucleus and the orbital electrons. This interaction is called Coulomb interaction. As a result of these interactions, the electrons can cause collision and radiation loss or be scattered. Energy losses are defined as stopping power while scattering is defined as scattering power [12].

There may be collisions between the incoming electron and the orbital electron or the nucleus of the atom. These collisions are called elastic or non-elastic collisions. In elastic collisions, the electron deviates from its own path. In non-elastic collisions, the electron deviates from its own path. Then, it transmits a portion of its energy to the orbital electron or it spreads in the form of a bremsstrahlung.

The interaction between an electron and an atom is shown in Figure 2.2, where a is the atomic radius and b is the impact parameter.

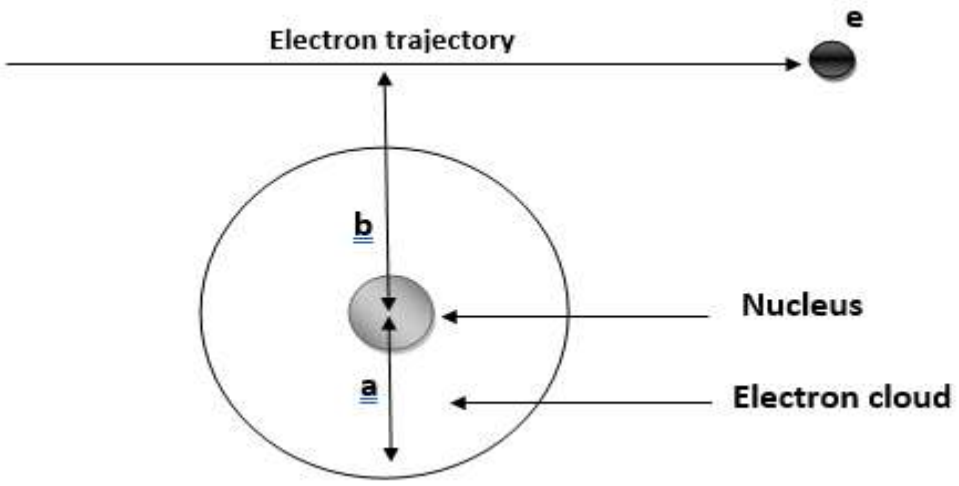

Figure 2.2 Interaction between an electron and an atom.

In Figure 2.2 ;

- When b is greater than a, the electron will cause a soft collision with the atom. As a result, the incoming electron will transmit very little energy to the electrons in the orbit.

- When b is equal to a, the electron causes a collision with the orbital electron. As a result, the incoming electron transfers a large part of its kinetic energy to the orbital electron.
- When b is less than a, the electron causes a radiative collision with the atomic nucleus. As a result, it emits a photon that has the energy between the kinetic energy of the incoming electron and zero. The radiated photon is called the bremsstrahlung photon. The energy of this photon is inversely proportional to the magnitude of the b (impact parameter). The smaller the b, the higher the energy of the photon [18].

There is non-elastic interaction between electrons and solids. The result of this interaction is very important for basic research and wide application areas. We can detect radiation by interacting with some materials. We can then investigate the change in the system configuration.

When the incoming electron has enough energy, it can break the weak connected electron. This causes ionization. A second ionization may occur if the removed electron still has sufficient energy. This process continues as long as the energy of the electron has enough energy [4]. However, all electrons has enough energy do not perform secondary ionization. The fact that an electron causes ionization depends on two characteristics. These are cross-sections depending on the type of target, atom and energy. Ionization of atoms has been investigated in many studies. Because, their use in physics research and materials is important. Electrons can affect the very deep of materials. Therefore, they can give us important information about the structure of materials. Symbolically, for an atom or a molecule Xq, with total positive charge q, the electron ionization process can be written as [4]

$$e + X_q \rightarrow X_{q+1} + 2e \tag{2.16}$$

In quantum electrodynamics, Moller scattering is said to occur due to the exchange of virtual photons between the electrons. In classical electrodynamic terms, it can be said that there is a result of Coulomb repulsion between the two electrons.

This refers to the elastic scattering of an electron from another electron (or a positron from another positron). The interaction can be symbolically described by [4]

$$e + e \rightarrow e + e \tag{2.17}$$

In terms of quantum electrodynamics, as with Moller scattering, Bhabha scattering is considered to be due to the exchange of virtual photons between an electron and a positron. Classically, it can be thought to occur because of the Coulomb attraction between the two particles. This is the scattering of an electron from a positron. The reaction can be written as [4]

$$e + e^{+} \rightarrow e + e^{+} \tag{2.18}$$

Another interaction mode is electron-positron annihilate. In this process, an electron and a positron annihilate each other's. They produce at least two photons, considering that the particles are initially at rest. It is a perfect example of the notion that mass can be converted into energy [4]. With this process, at very high energies (several GeV), the annihilation process can be produced quarks form mesons.

A charged particle can be slowed or accelerated by electromagnetic or different charged particles. This movement consists of electromagnetic radiation. This is called bremsstrahlung. According to the classical theory, the charged particles that are accelerated or slowed down need to emit energy.

The bremsstrahlung has two important examples. Firstly, deceleration of charged particles. When charged particles enter a material they are decelerated by the electric field of the atomic nuclei and atomic electrons. Secondly, acceleration of charged particles. When ultra-relativistic charged particles move through magnetic fields they are forced to move along a curved path. Since their direction of motion is continually changing, they are also accelerating and so emit bremsstrahlung.

Bremsstrahlung is very strong if the particles are light. This is very important for beta particles. Because the energy loss due to the bremsstrahlung in the energies below 1 MeV is very small.

2.6.1 Electron–Orbital Electron Interactions (Collisional Stopping Power)

Coulomb interactions between electrons and orbital electrons occur. As a result of this interaction, the atom is ionized and excited. In the ionization, the orbital electron is removed from the atom. In excitation, the orbital electron is transferred to a higher orbit. As a result of atomic excitation and ionization, energy losses occur. These energy losses are defined as ionization (collision) stopping power. The electronic stopping power for electrons is written as [3,16,19]:

$$S^{\mp}_{electronic} = -\left(\frac{dE}{dx}\right)_{electronic} = \frac{2\pi r_e^2 m_0 c^2}{\beta_e^2}\frac{\rho Z N_A}{A}\ln\frac{T^2}{I} + \ln 1 + \frac{\tau}{2} + F^{\mp}(\tau) - \delta \quad (2.19)$$

$$F^{-}(\tau) = (1-\beta_e^2)\left(1+\frac{\tau^2}{8}-(2\tau+1)\ln 2\right) \quad \text{for electrons} \quad (2.20)$$

$$F^{+}(\tau) = 2\ln 2 - \frac{\beta_e^2}{12}\left(23+\frac{14}{\tau+2}+\frac{10}{(\tau+2)^2}+\frac{4}{(\tau+2)^3}\right) \quad \text{for positrons} \quad (2.21)$$

where $\beta_e = \sqrt{1-\left(\frac{m_0c^2}{T+m_0c^2}\right)^2}$ is a correction factor for electrons, $\tau = \frac{T}{m_0c^2}$ is the ratio of the electron relativistic energy to its rest mass energy, T is the kinetic energy of beta particle, δ is a density-effect correction, and I is the mean ionization energy.

2.6.2 Electron–Nucleus Interaction (Radiative Stopping Power)

Coulomb interactions occur between the incoming electron and the atomic nucleus. As a result of this interaction, X-ray photons (bremsstrahlung) are produced. It causes the scattering of the electron and the energy loss of the electron. This type of energy loss is defined as radiative stopping power.

The energy loss by radiation and the radiative yield increase directly with the absorber atomic number Z and the kinetic energy of electrons. The radiative stopping power is [16,19]

$$S_{radiative} = \left(-\frac{dE}{dx}\right)_{radiative} = \frac{(Z+1)Ze^4\rho T}{137\, m_0^2c^4}\left[4\ln\left(\frac{2T}{m_0c^2}\right)-\frac{4}{3}\right] \quad (2.22)$$

2.6.3 The Total Stopping Power and Range

Stopping power is defined as the energy loss per unit distance. Compared to heavily charged particles, electrons behave quite differently as they pass through the substance. The main reason for this is the very small mass of electrons as compared to heavy charged particles. Because of their low mass, the electrons move so fast that their velocities can be very close to the speed of light. Since in such a situation, the relativistic effects must be considered to deduce meaningful results, the computations become more complicated than for the heavy charged particles [16,19].

$$\left(-\frac{dE}{dx}\right)_{electron} = S_{electronic} + S_{radiative} \tag{2.23}$$

Ignoring the radiative part for lower energy range, collision energy loss of the electrons is very important. Stopping powers calculated from the relativistic Bethe equation [3,16,19]

$$S = \frac{2\pi r_e^2 m_0 c^2}{\beta_e^2}\frac{\rho Z N_A}{A}\left[\ln\left(\frac{T}{I}\right)^2 + \ln\left(1+\frac{\tau}{2}\right) + F(\tau) - \delta\right] \tag{2.24}$$

We have assumed δ to be zero here since its inclusion leads, for our energy range, to a correction of less than 0.3%.

The mean ionization energy was calculated with an formula [19, 20],

$$I = \begin{cases} [12 + 7(Z^{-1})]Z & eV \quad Z < 13 \\ [9.76 + 58.8(Z^{-1.19})]Z & eV \quad Z \geq 13 \end{cases} \tag{2.25}$$

with values of the constants inserted, Eq.(2.24) becomes

$$S = \frac{0.15307\ Z\rho}{\beta_e^2 A}\left[\ln\left(\frac{T}{I}\right)^2 + \ln\left(1+\frac{\tau}{2}\right) + F(\tau)\right] \tag{2.26}$$

All of these expressions for the stopping power only apply to pure chemical elements. The stopping power of a compound or any complicated mixture will depend on the overall density and the relative numbers of electrons from each chemical element. The average (mean) mass stopping power (S/ρ) is [19]

$$\left(\frac{S}{\rho}\right) = w_1\left(\frac{S}{\rho}\right)_1 + w_2\left(\frac{S}{\rho}\right)_2 + w_3\left(\frac{S}{\rho}\right)_3 + \cdots \quad (2.27)$$

where w_1 is the fraction by mass of element 1 in the entire mixture. The unit of mass stoppig power is usually expressed as Mev.cm^2/g.

The most suitable phosphorus layer must have some properties. They should be of sufficient thickness to absorb most of the beta particles and allow high-efficiency transfer of the emitted luminescence. The relationship of the beta range and the phosphor layer thickness is the key to optimizing beta radioluminescence nuclear battery. The beta range was calculated with an emperical formula [20, 21],

$$R(T) = \int_0^T [S_{col}(T) + S_{rad}(T)]^{-1} dT \quad (2.28)$$

$$R = \frac{0.412 E_{max}^{1.265 - 0.0954 \ln E_{max}}}{\rho} \qquad E_{max} \leq 2.5 \text{ MeV} \quad (2.29)$$

where R is the beta range in the phosphor layers (cm), E_{max} is the maximum kinetic energy of the beta source (MeV), and ρ is density of the phosphors (g/cm^3).

2.7 Generation Rate

Generation rate is the number of electron hole pairs in phosphors due to beta particles that is used for p-n or other types of junctions in beta voltaics. g(R) is the electron-hole generation rate, if the flux of beta particles a range R from the junction is f(R), then [22]

$$g(R) = -\frac{E_{mean}}{\varepsilon}\frac{df(R)}{dR} \quad (2.30)$$

$$\varepsilon = 2.8E_g + 0.5 \quad (2.31)$$

where E_g is the bandgap energy of the phosphors mixture.

$$f(R) = \Phi(1 - r)e^{-\alpha R} \quad (2.32)$$

$$g(R) = \frac{E_{mean}\Phi\alpha}{\varepsilon}(1 - r)e^{-\alpha R} \quad (2.33)$$

where E_{mean} is the mean (average) kinetic energy of the beta particle (MeV) and ε is the average energy expended in producing an electron hole pair [23,24]. It is assumed that the beta particles are absorbed exponentially with an absorption coefficient α, Φ is the incident beta flux (1mCi/cm^2), R is the range and r is the beta reflection coefficient.

CHAPTER 3

PROPERTIES OF PHOSPHORESCENT MATERIALS

In this part basic information about the phosphorescent material is given starting from the luminescence theory.

3.1 Luminescence Mechanism

Luminescence is a general term to describe the process in which a material absorbs energy from an external source and re-emits that energy in the form of visible light [25]. Luminescence can be categorized according to the source of excitation [26]:

(a) photoluminescence is caused by the absorption of light or photons.
(b) radioluminescence is caused by the action of high-energy particles from cosmic rays, radioactive materials and accelerators.
(c) electroluminescence is caused by the creation of an electric field.
(d)mechano or triboluminescence is caused by mechanical force.
(e) cathodoluminescence is caused by cathode rays or electrons,
(f) chemiluminescence is caused by chemical operates.
(g) sonoluminescence is caused by high frequency sound waves or phonons, and bioluminescence is caused by biological operates.

There are two steps for luminescence emission. These are emission and excitation processes. Excitation, where by the system temporarily attains a higher energy state. Emission, in which absorbed energy is released by radiative or non-radiative transitions [26].

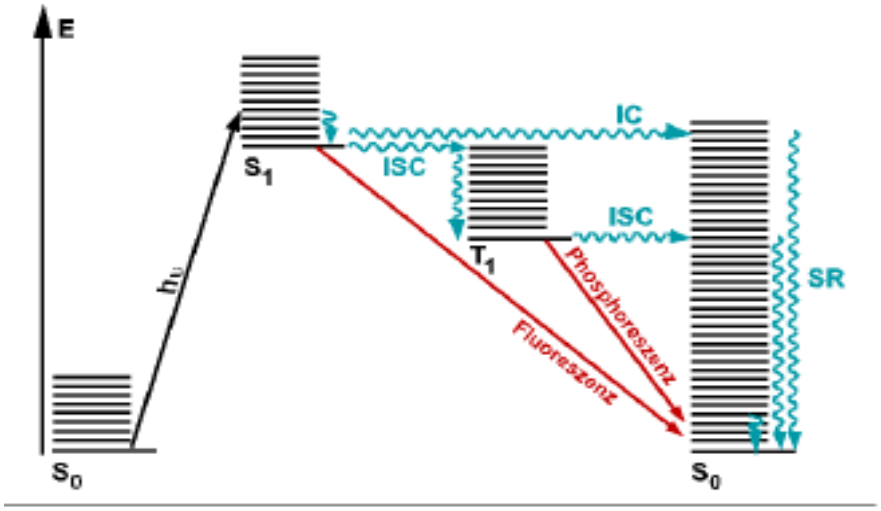

Figure 3.1 The luminescence processes according to the Jablonski diagram

When we examine the luminescence processes according to the Jablonski diagram in the Figure 3.1 [27];

- An electron in the ground state S_0 is activated to an excited state S_1 by the impact of energy.
- The excited state of the electron has a higher energy and is only stable for a short time until the electron goes back to the ground state S_0.
- The energy difference between these two states is released in form of a light emission.

Phosphorescence and fluorescence terms are related to each others. Both processes belong to the same type of photoluminescence. Fluorescence is a process where the excitation energy is absorbed from a source of light meaning a photon and the released energy is a photon, too. Unlike fluorescence, a phosphorescent material does not immediately reemit the radiation it absorbs. Phosphorescence is a process in which the energy absorbed by the substance is released slowly in the light. This is a mechanism used for shining materials in the dark. These substances store energy for a long time [28]. The electron from the excited state S_1 changes its spin and goes to a forbidden energy state T_1: Inter system crossing (ISC). There is no light emission while the ISC.

The electron from the T_1 state falls back to ground state and emits light. This process takes longer than fluorescence because the electron has to change its spin again when it returns from T_1 to S_0.

Fluorescence is light emitted over 10^{-8} seconds. It consists of an excited single state. Phosphorescence is spread in more than 10^{-8} seconds. This is propagated from excited triplet state. Fluorescence is independent of temperature but phosphorescence depends on temperature. Fluorescence occurs in simple or complex gas, liquid and solid chemical systems.

3.2 Radioluminescence Theory and RL Batteries

It is a kind of luminescence produced by the effect of high energy particles coming from accelerators, cosmic rays, radioactive materials or other sources. Radioactive elements can emit radiation from alpha particles, electrons and gamma rays. Luminescence occurs in the substances which are stimulated by the effect of these elements.

This luminescence is called radioluminescence. When a luminescent crystal is bombarded with alpha particles, the luminescence can be observed under a microscope. The phosphorescence dyes used in the dials of clocks and similar devices are a mixture of a phosphorescence substance and a radioactive substance.

Polar light is the most striking example of radioluminescence observed in nature. Huge amounts of electrons and ions as a result of radioactive processes in the Sun are released into space by the solar wind. When they approach the Earth, the discharge processes of these particles accumulated in the upper atmosphere by the effect of the magnetic field of the Earth cause the luminescence phenomenon known as polar light [29].

Indirect conversion radioluminescence batteries performs electrical conversion in two stages. These stages can be listed as follows;
1) produce luminescence by radioactive decay,
2) to provide a potential difference with the help of PV cells.

These batteries are very suitable for condensing radiation. In addition, it allows applications of high energy particles. The inadequacy of studies on power outputs is a disadvantage.

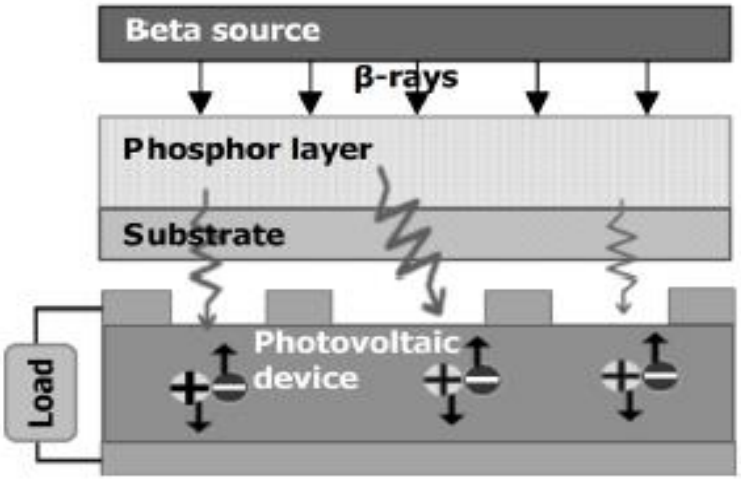

Figure 3.2 Schematics of a beta RL nuclear battery [20]

The optimal phosphor layer must be of sufficient thickness to absorb most of beta particles and still allow for high-efficient transmission of the emitted luminescence. The relationship of the beta range and the phosphor layer thickness is the key to optimizing beta radio-luminescence nuclear battery [20].

CHAPTER 4

CALCULATIONS AND RESULTS

In this chapter, we concentrate on the analysis of parameters that are given in chapter 3 for different compounds of Zn and Sr phosphors. Such phosphors are used in the development of indirect energy conversion betavoltaic batteries.

4.1 Mass Stopping Power and Range Analysis

In this section we have calculated the mass stopping power and range values from the Eqn. (2.26), Eqn. (2.27), and Eqn. (2.29) for different compounds of Zn and Sr by using the density values given in Table 4.1 [30-32]. These values are given in Table 4.2, Table 4.3 Table 4.4, Table 4,5 Table 4.6, Table 4.7, Table 4.8, and Table 4.9.

Table 4.1 Density for used phosphorescent materials [30-32].

Density (g/cm^3)			
ZnS:CuCl	1.78	**$SrAl_2O_4:Eu^{2+},Dy^{3+}$**	3.569
ZnS	4.09	**$SrB_4O_7:Sm^{2+}$**	4.02
ZnO	5.606	**$SrGa_2S_4:Eu$**	3.59
$Zn_2SiO_4:Mn^{2+}$	4.25	**$Sr_4Al_{14}O_{25}:Eu$**	3.66

Table 4.2 The mass stopping power and range according to the energy values in the range of 0-1 MeV for ZnS:ClCu.

Energy (MeV)	**Mass Stopping Power ($Mev.cm^2/g$)**	**Range (cm)**
0.05	5.95131	0.00222254
0.1	4.30867	0.00758247
0.15	3.66838	0.0148976
0.2	3.33467	0.0236026
0.25	3.13673	0.0333616
0.3	3.01089	0.043952
0.35	2.92778	0.0552154
0.4	2.87193	0.0670344
0.45	2.83439	0.0793183
0.5	2.80964	0.0919959
0.55	2.79411	0.105009
0.6	2.78537	0.118312
0.65	2.78172	0.131863
0.7	2.78195	0.145632
0.75	2.78517	0.159588
0.8	2.79072	0.173709
0.85	2.79807	0.187974
0.9	2.80686	0.202364
0.95	2.81677	0.216865
1	2.82756	0.231461

Table 4.3 The mass stopping power and range according to the energy values in the range of 0-1 MeV for ZnS.

Energy (MeV)	**Mass Stopping Power ($Mev.cm^2/g$)**	**Range (cm)**
0.05	5.98445	0.000967266
0.1	4.33356	0.00329995
0.15	3.68996	0.00648357
0.2	3.35452	0.010272
0.25	3.15555	0.0145192
0.3	3.02908	0.0191282
0.35	2.94556	0.0240302
0.4	2.88944	0.0291739
0.45	2.85174	0.03452
0.5	2.8269	0.0400373
0.55	2.81133	0.0457009
0.6	2.80257	0.0514901
0.65	2.79894	0.0573879
0.7	2.79921	0.06338
0.75	2.80249	0.069454
0.8	2.8081	0.0755996
0.85	2.81553	0.0818078
0.9	2.8244	0.0880706
0.95	2.8344	0.0943811
1	2.84528	0.100733

Table 4.4 The mass stopping power and range according to the energy values in the range of 0-1 MeV for ZnO.

Energy (MeV)	**Mass Stopping Power (Mev.cm^2/g)**	**Range (cm)**
0.05	6.08061	0.000705693
0.1	4.38723	0.00240756
0.15	3.72923	0.00473025
0.2	3.38654	0.00749423
0.25	3.1832	0.0105929
0.3	3.05379	0.0139555
0.35	2.96816	0.0175318
0.4	2.91045	0.0212845
0.45	2.87148	0.0251849
0.5	2.84563	0.0292102
0.55	2.82921	0.0333422
0.6	2.81974	0.0375659
0.65	2.8155	0.0418688
0.7	2.81524	0.0462405
0.75	2.81804	0.050672
0.8	2.82323	0.0551556
0.85	2.83028	0.0596849
0.9	2.83881	0.0642541
0.95	2.84849	0.0688582
1	2.85908	0.0734927

Table 4.5 The mass stopping power and range according to the energy values in the range of 0-1 MeV for $Zn_2SiO_4:Mn^{2+}$.

Energy (MeV)	**Mass Stopping Power ($Mev.cm^2/g$)**	**Range (cm)**
0.05	6.46216	0.000930851
0.1	4.63649	0.00317572
0.15	3.93028	0.00623948
0.2	3.56281	0.00988533
0.25	3.34459	0.0139726
0.3	3.20542	0.0184081
0.35	3.11302	0.0231255
0.4	3.05042	0.0280756
0.45	3.00783	0.0332204
0.5	2.97923	0.03853
0.55	2.96071	0.0439804
0.6	2.94962	0.0495517
0.65	2.94411	0.0552275
0.7	2.94286	0.0609939
0.75	2.94489	0.0668393
0.8	2.94949	0.0727535
0.85	2.95609	0.0787279
0.9	2.96428	0.084755
0.95	2.97372	0.090828
1	2.98415	0.0969412

Table 4.6 The mass stopping power and range according to the energy values in the range of 0-1 MeV for $SrAl_2O_4:Eu^{2+},Dy^{3+}$.

Energy (MeV)	**Mass Stopping Power ($Mev.cm^2/g$)**	**Range (cm)**
0.05	4.80554	0.00111127
0.1	3.52725	0.00379123
0.15	3.02385	0.00744882
0.2	2.76111	0.0118013
0.25	2.60573	0.0166808
0.3	2.50761	0.021976
0.35	2.44349	0.0276077
0.4	2.40108	0.0335172
0.45	2.37328	0.0396592
0.5	2.35567	0.0459979
0.55	2.3454	0.0525047
0.6	2.34051	0.0591558
0.65	2.33967	0.0659317
0.7	2.3419	0.0728158
0.75	2.34647	0.0797941
0.8	2.35287	0.0868546
0.85	2.36068	0.093987
0.9	2.3696	0.101182
0.95	2.37937	0.108432
1	2.38982	0.11573

Table 4.7 The mass stopping power and range according to the energy values in the range of 0-1 MeV for $SrB_4O_7:Sm^{2+}$.

Energy (MeV)	**Mass Stopping Power ($Mev.cm^2/g$)**	**Range (cm)**
0.05	5.99615	0.000984109
0.1	4.3042	0.00335741
0.15	3.65019	0.00659647
0.2	3.31005	0.0104509
0.25	3.1082	0.0147721
0.3	2.9796	0.0194613
0.35	2.89431	0.0244486
0.4	2.83663	0.0296819
0.45	2.79749	0.0351211
0.5	2.77131	0.0407345
0.55	2.75446	0.0464967
0.6	2.74448	0.0523867
0.65	2.73967	0.0583872
0.7	2.7388	0.0644836
0.75	2.74097	0.0706634
0.8	2.7455	0.0769161
0.85	2.75189	0.0832323
0.9	2.75974	0.0896041
0.95	2.76874	0.0960246
1	2.77865	0.102488

Table 4.8 The mass stopping power and range according to the energy values in the range of 0-1 MeV for $SrGa_2S_4$:Eu.

Energy (MeV)	**Mass Stopping Power ($Mev.cm^2/g$)**	**Range (cm)**
0.05	5.14161	0.00110198
0.1	3.76368	0.00375955
0.15	3.22183	0.00738657
0.2	2.93901	0.0117027
0.25	2.7716	0.0165414
0.3	2.66568	0.0217923
0.35	2.59627	0.027377
0.4	2.55018	0.0332371
0.45	2.51976	0.0393278
0.5	2.5003	0.0456135
0.55	2.4887	0.0520659
0.6	2.4829	0.0586615
0.65	2.48145	0.0653807
0.7	2.4833	0.0722073
0.75	2.48767	0.0791273
0.8	2.49402	0.0861288
0.85	2.50189	0.0932016
0.9	2.51095	0.100337
0.95	2.52095	0.107526
1	2.53167	0.114763

Table 4.9 The mass stopping power and range according to the energy values in the range of 0-1 MeV for $Sr_4Al_{14}O_{25}$:Eu.

Energy (MeV)	Mass Stopping Power ($Mev.cm^2/g$)	Range (cm)
0.05	6.64266	0.00108091
0.1	4.74309	0.00368765
0.15	4.01134	0.0072453
0.2	3.63094	0.0114789
0.25	3.40495	0.0162251
0.3	3.2606	0.0213755
0.35	3.16452	0.0268534
0.4	3.09917	0.0326014
0.45	3.05447	0.0385756
0.5	3.02419	0.0447412
0.55	3.0043	0.0510701
0.6	2.99208	0.0575395
0.65	2.98562	0.0641302
0.7	2.98357	0.0708263
0.75	2.98491	0.0776139
0.8	2.98891	0.0844816
0.85	2.99498	0.0914191
0.9	3.0027	0.0984176
0.95	3.01173	0.10547
1	3.02178	0.112568

From the analysis of mass stopping power and range given above tables, it is seen that the stopping power decreases when energy increases, but in the vicinity of 0.75 MeV, these values starts to begin increase slowly and range is directly proportional to the energy values. The graphs of the mass stopping power respect to the energy values are given in Figure 4.1, Figure 4.2, Figure 4.3, and Figure 4.4.

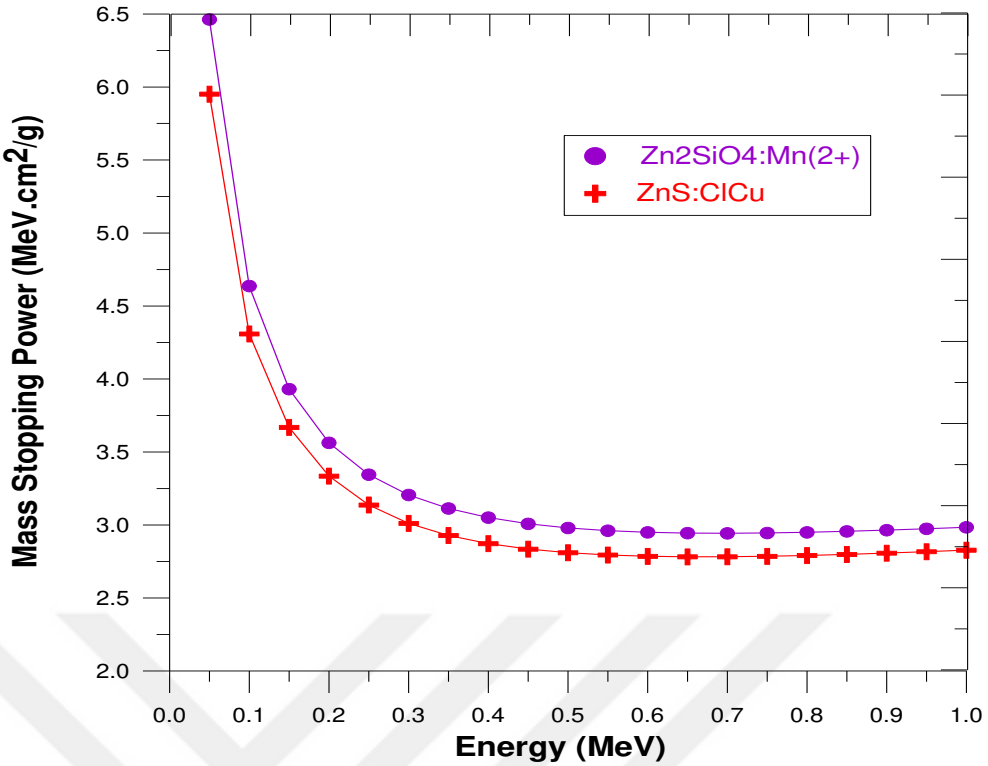

Figure 4.1 The graph of the mass stopping power according to the energy values in the range of 0-1 MeV for ZnS:ClCu and $Zn_2SiO_4:Mn^{2+}$.

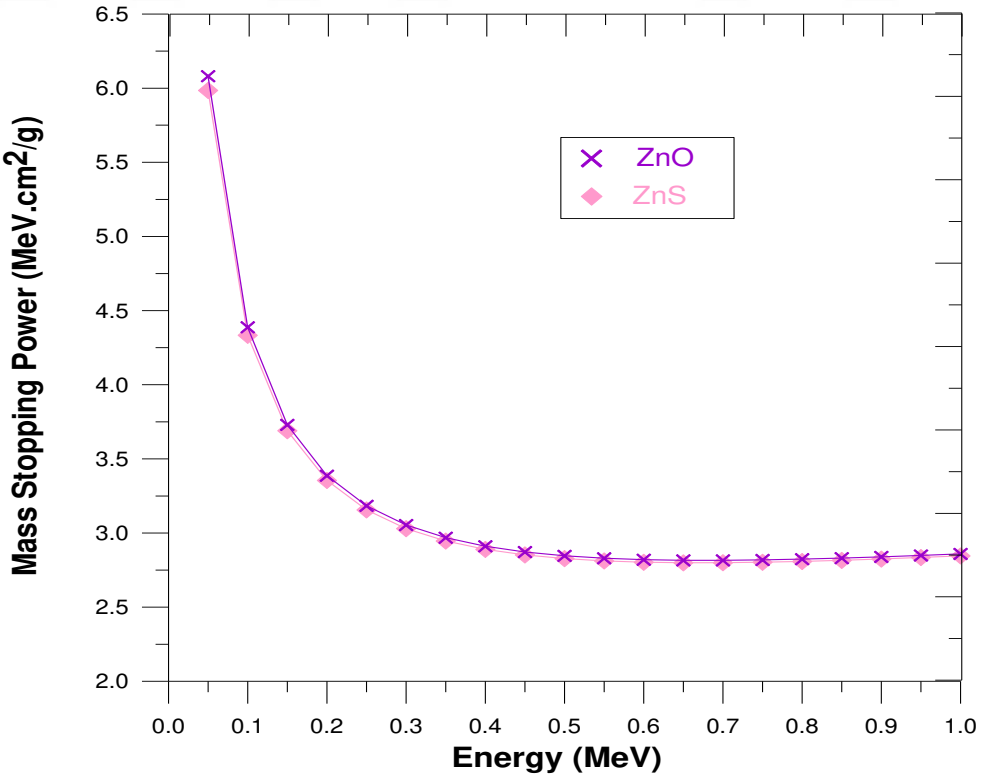

Figure 4.2 The graph of the mass stopping power according to the energy values in the range of 0-1 MeV for ZnO and ZnS.

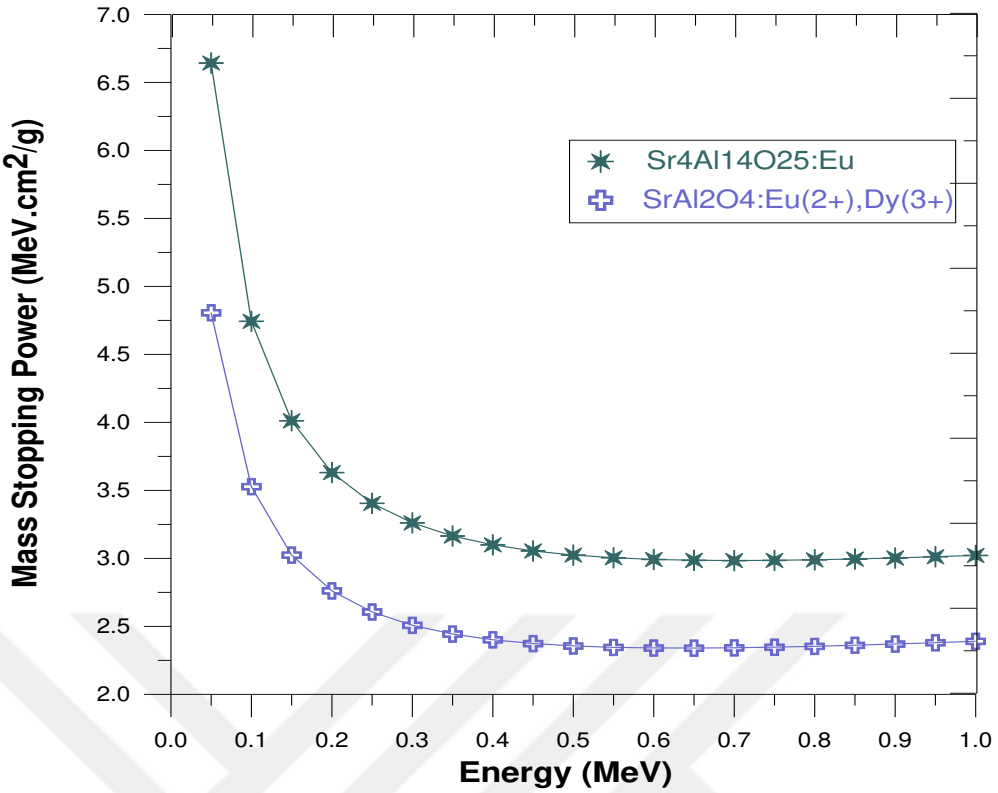

Figure 4.3 The graph of the mass stopping power according to the energy values in the range of 0-1 MeV for $Sr_4Al_{14}O_{25}$:Eu and $SrAl_2O_4$:Eu^{2+},Dy^{3+}.

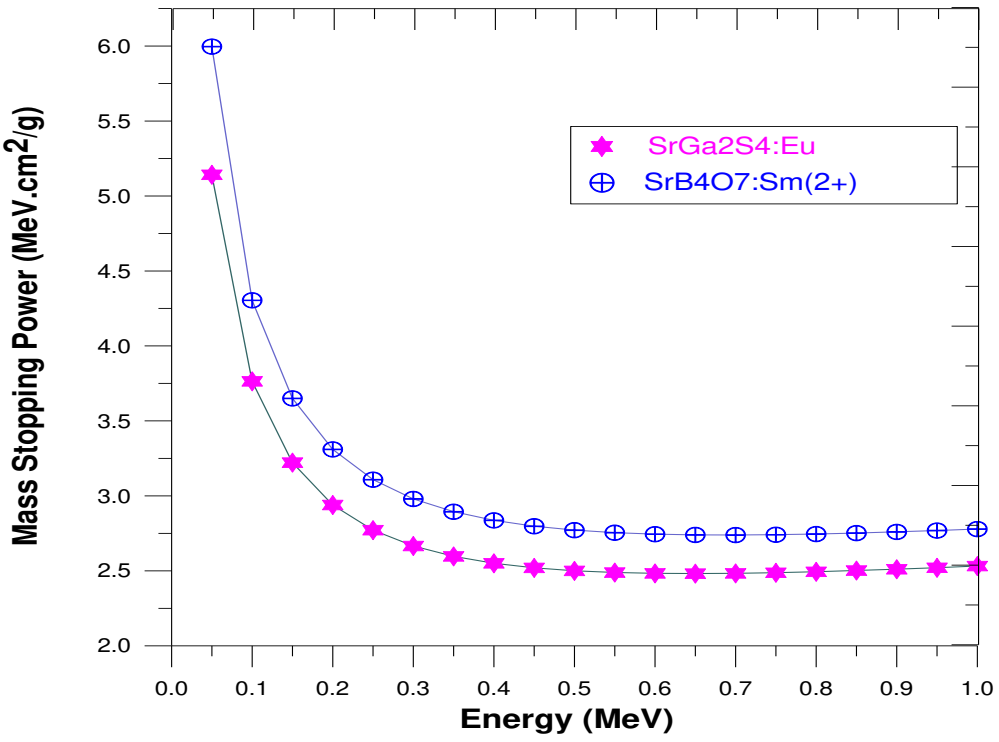

Figure 4.4 The graph of the mass stopping power according to the energy values in the range of 0-1 MeV for $SrGa_2S_4$:Eu and SrB_4O_7:Sm^{2+}.

Table 4.10 Kinetic energy values of the used beta particles [21]

	Mean Kinetic Energy (E_{mean}) (MeV)	**Maximum Kinetic Energy (E_{max}) (MeV)**
H-3(T)	0.005686	0.018601
Pm147	0.061960	0.224700
Ni-63	0.017130	0.065870
Sr-90	0.195800	0.546000
C-14	0.049470	0.156480
Zr-93	0.019500	0.061531

In Table 4.11 a specific calculation of mass stopping power for a different beta sources are given based on maximum kinetic energies given in Table 4.10 [21].

Table 4.11 The mass stopping power values based on the maximum kinetic energies of the beta isotopes for phosphor mixtures.

Mass Stopping Power (Mev.cm^2/g)						
	H-3 (T)	**Pm-147**	**Ni-63**	**Sr-90**	**C-14**	**Zr-93**
ZnS:CuCl	9.73832	3.2251	5.20727	2.79508	3.61341	5.37948
ZnS	9.78878	3.24438	5.23672	2.81229	3.63471	5.4098
ZnO	10.0214	3.274	5.31254	2.83024	3.67278	5.49016
$Zn_2SiO_4:Mn^{2+}$	10.7667	3.44207	5.63246	2.96189	3.86975	5.82408
$SrAl_2O_4:Eu^{2+},Dy^{3+}$	7.6656	2.67501	4.22919	2.346	2.98056	4.36299
$SrB_4O_7:Sm^{2+}$	9.99612	3.19835	5.22701	2.75552	3.59414	5.40461
$SrGa_2S_4:Eu$	8.23668	2.84626	4.5199	2.48939	3.17524	4.66417
$Sr_4Al_{14}O_{25}:Eu$	11.1758	3.50593	5.77783	3.00558	3.94868	5.97732

In our results, we observed that mass stopping power is inversely proportional to maximum kinetic energy of the beta source. From the above table, it is concluded that $SrAl_2O_4:Eu^{2+},Dy^{3+}$ has high mass stopping power value compared to other phosphor compounds depending on energy of the beta source.

The graphs of range values for some phosphors are given in Figure 4.5, Figure 4.6, Figure 4.7, and Figure 4.8.

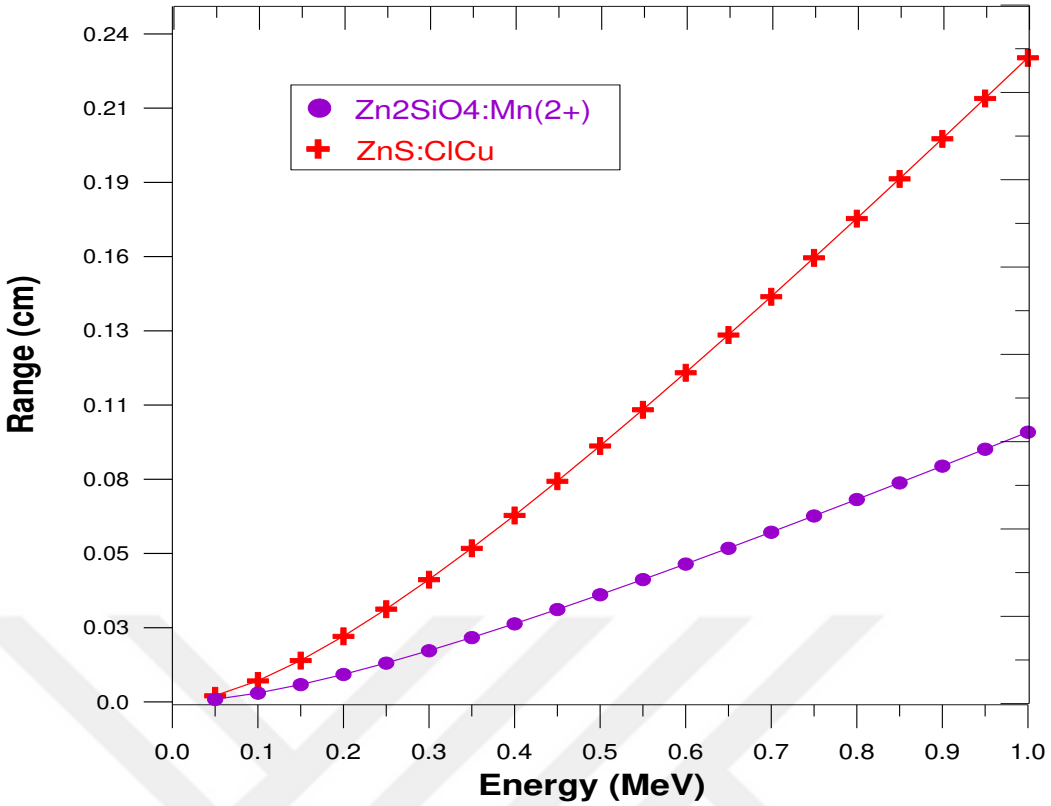

Figure 4.5 The graph of the range according to the energy values in the range of 0-1 MeV for ZnS:ClCu and $Zn_2SiO_4:Mn^{2+}$.

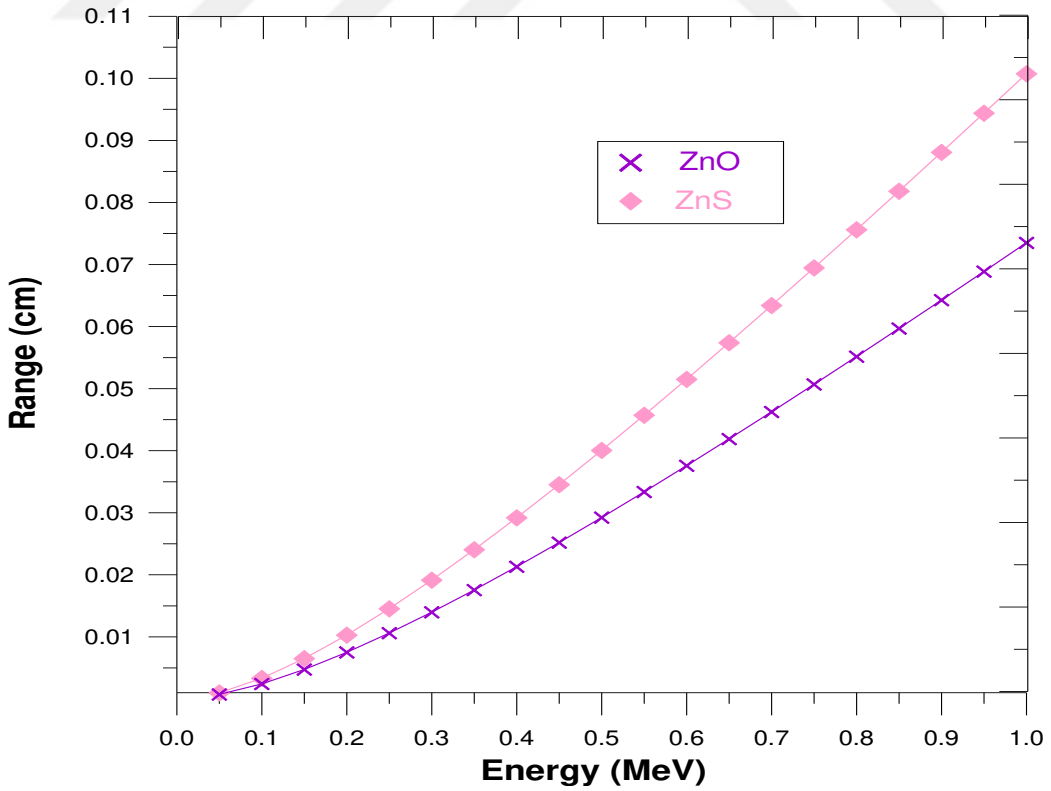

Figure 4.6 The graph of the range according to the energy values in the range of 0-1 MeV for ZnO and ZnS.

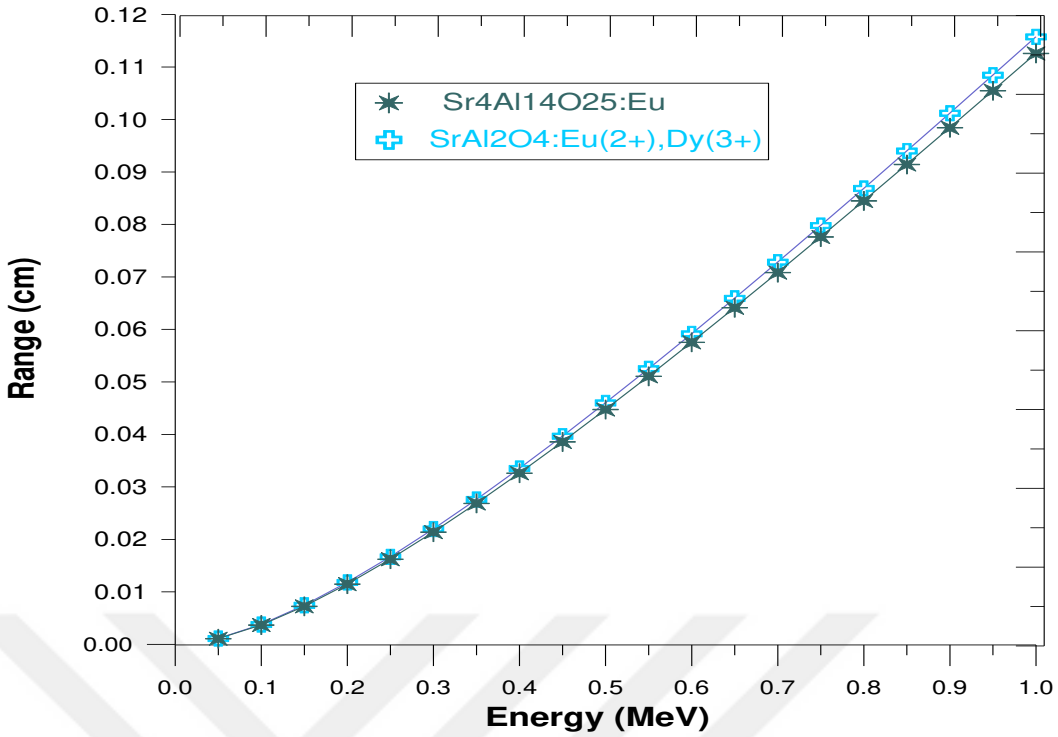

Figure 4.7 The graph of the range according to the energy values in the range of 0-1 MeV for $Sr_4Al_{14}O_{25}$:Eu and $SrAl_2O_4$:Eu^{2+},Dy^{3+}.

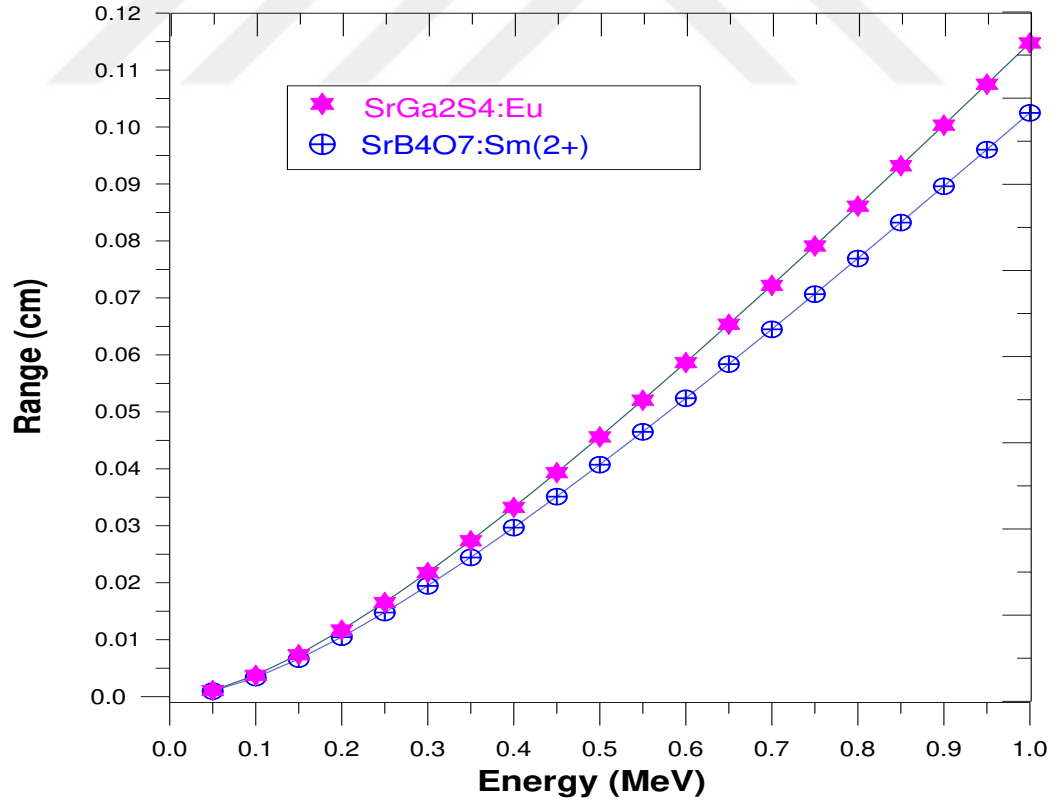

Figure 4.8 The graph of the range according to the energy values in the range of 0-1 MeV for $SrGa_2S_4$:Eu and SrB_4O_7:Sm^{2+}.

The range values for each phosphor are also calculated by using maximum kinetic energy values of beta sources given in Table 4.12 and density values given in Table 4.1.

Table 4.12 The range values based on the maximum kinetic energies of the beta isotopes for phosphor mixtures.

	Range (cm)					
	H-3 (T)	**Pm-147**	**Ni-63**	**Sr-90**	**C-14**	**Zr-93**
ZnS:CuCl	0.0003293	0.02830	0.003660	0.1039	0.01595	0.003240
ZnS	0.0001433	0.01231	0.001593	0.04524	0.006944	0.001410
ZnO	0.0001045	0.00898	0.001162	0.03300	0.005066	0.001028
$Zn_2SiO_4:Mn^{2+}$	0.0001379	0.01185	0.001533	0.04353	0.006682	0.001357
$SrAl_2O_4:Eu^{2+},Dy^{3+}$	0.0001646	0.01415	0.001830	0.05197	0.007978	0.001620
$SrB_4O_7:Sm^{2+}$	0.0001458	0.01253	0.001620	0.0460	0.007065	0.001434
$SrGa_2S_4:Eu$	0.0001632	0.01403	0.001815	0.0515	0.007911	0.001606
$Sr_4Al_{14}O_{25}:Eu$	0.0001601	0.01376	0.001780	0.05055	0.007760	0.001575

In our results, we observed that range is directly proportional to the energy but it is inversely proportional to the density of the phosphors. These values corresponds to the thickness of phosphor compounds for RL betavoltaic battery design.

4.2 Generation Rate Analysis

Generation rate is an important parameter in indirect energy conversion betavoltaics. It gives total number of electron-hole pairs per unit volume entering cell (p-n or other type of junctions).

Before calculation of generation rate, we should calculate the absorption and reflection coefficient of these phosphors by using bandgap and average energy values listed in Table 4.13 [33-36].

Table 4.13 Bandgap energy and average energy expended in producing an electron-hole pair for phosphor mixtures [33-36].

	Bandgap Energy (eV)	**ε (eV)**
ZnS:CuCl	3.63	10.664
ZnS	3.75	11
ZnO	3.437	10.1236
$Zn_2SiO_4:Mn^{2+}$	5.5	15.9
$SrAl_2O_4:Eu^{2+},Dy^{3+}$	6.5	18.7
$SrB_4O_7:Sm^{2+}$	4.2	12.26

4.2.1 Absorption Coefficient

The linear absorption coefficient (α) determines how far into a material light or particle of a particular wavelength can penetrate before it is absorbed. The absorption coefficient depends on the material and also on the wavelength of light or particle which is being absorbed [37]:

$$\alpha = \mu_m \times \rho \tag{4.1}$$

Here α is in cm^{-1} and ρ is the material density given in Table 4.1, and μ_m, the mass attenuation coefficient is given by [5, 22, 37]

$$\mu_m = \frac{0.017}{E_{max}^{1.43}} \tag{4.2}$$

where μ_m is in cm^2g^{-1} and E_{max} (Mev) is given Table 4.10, the maximum kinetic energy of beta particle. The factor α describes the decay of excess concentration of electron hole pairs generated by beta electrons.

Absorption coefficient calculations are done for different Zn and Sr materials using Eqn. (4.1), and Eqn. (4.2). The graphs of the absorption coefficient with respect to the energy values are given in Figure 4.9, Figure 4.10, Figure 4.11, and Figure 4.12.

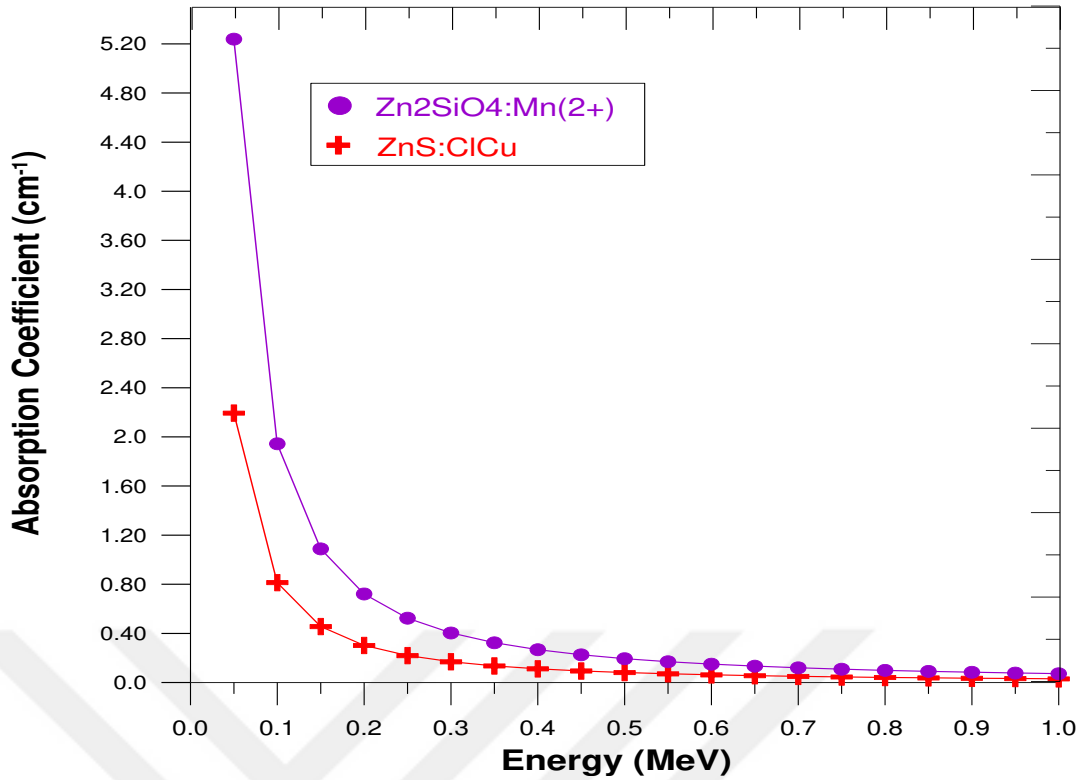

Figure 4.9 The graph of the absorption coefficient according to the energy values in the range of 0-1 MeV for ZnS:ClCu and $Zn_2SiO_4:Mn^{2+}$.

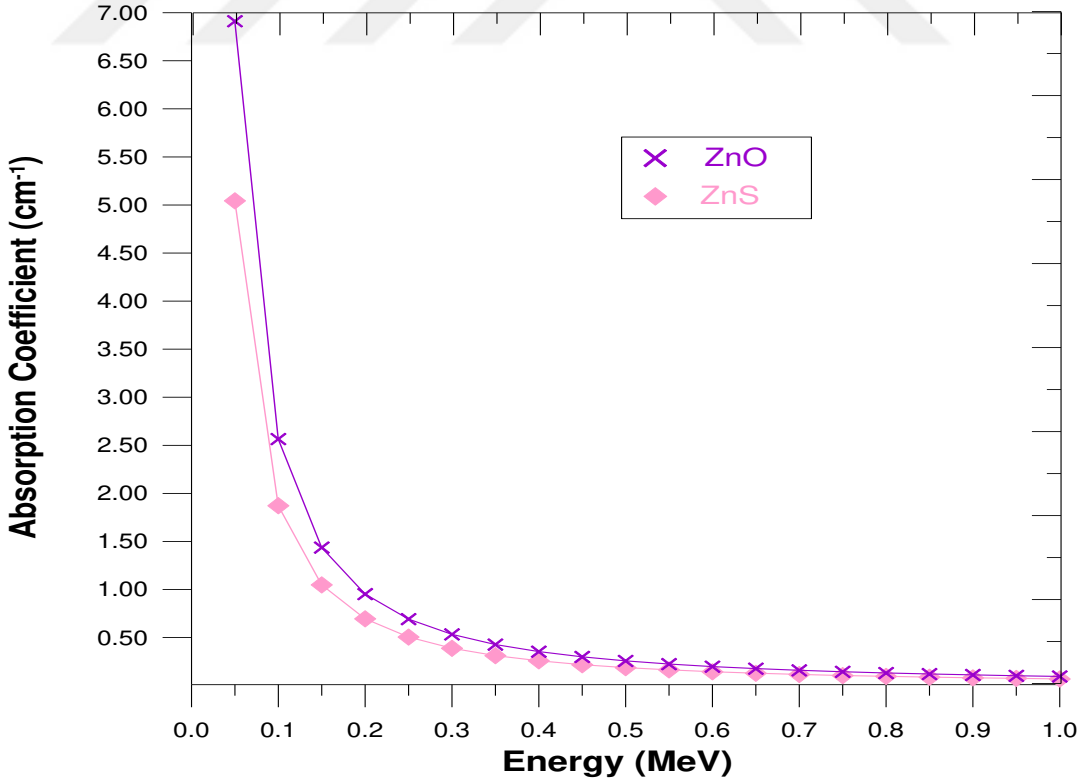

Figure 4.10 The graph of the absorption coefficient according to the energy values in the range of 0-1 MeV for ZnO and ZnS.

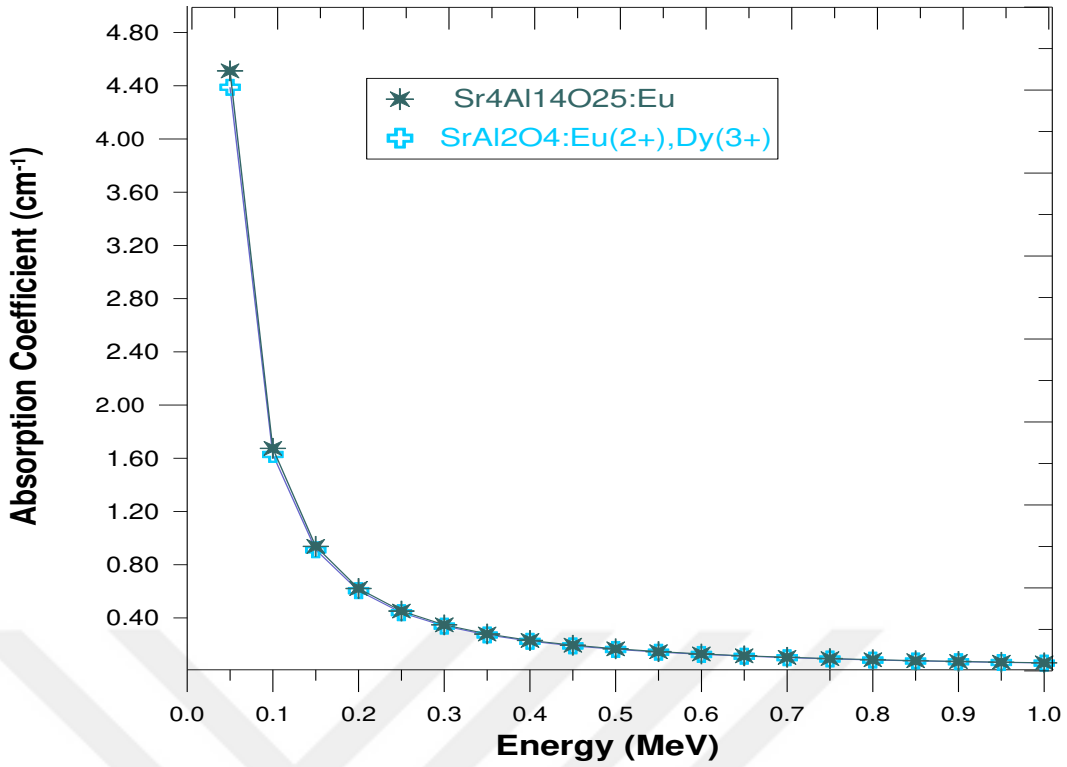

Figure 4.11 The graph of the absorption coefficient according to the energy values in the range of 0-1 MeV for $Sr_4Al_{14}O_{25}$:Eu and $SrAl_2O_4$:Eu^{2+},Dy^{3+}.

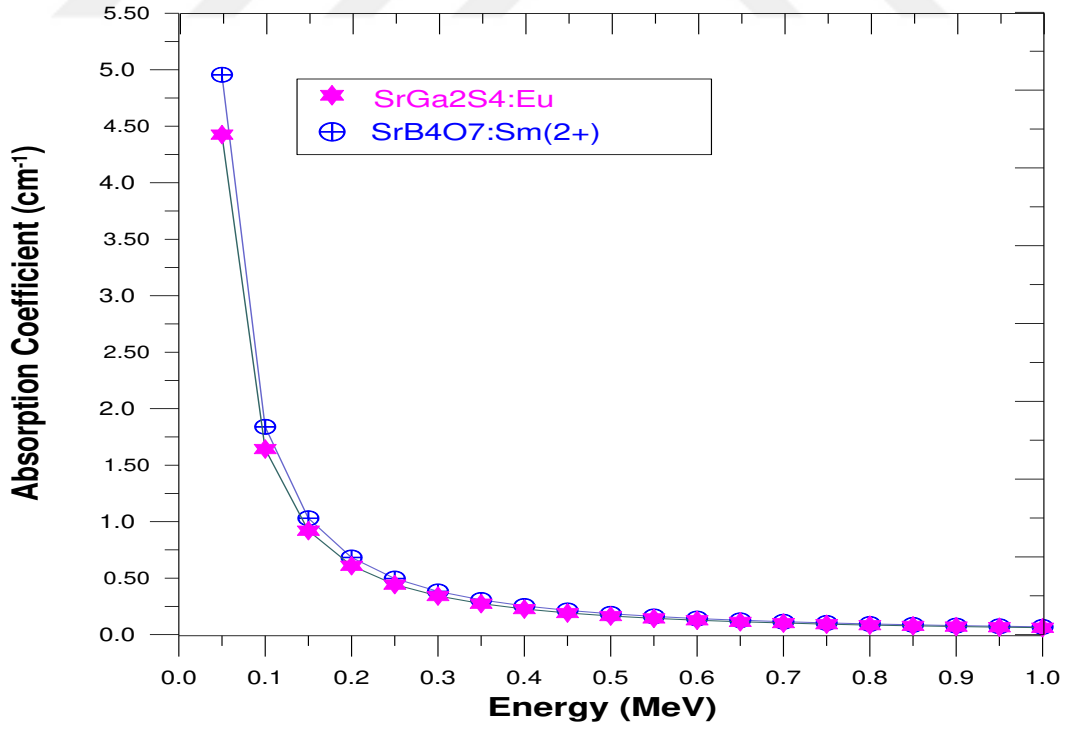

Figure 4.12 The graph of the absorption coefficient according to the energy values in the range of 0-1 MeV for $SrGa_2S_4$:Eu and SrB_4O_7:Sm^{2+}.

In Table 4.14 a specific calculation of the absorption coefficient for a different beta sources are given based on the maximum kinetic energies given in Table 4.10.

Table 4.14 The absorption coefficient based on the maximum kinetic energies of the beta isotopes for phosphor mixtures.

Absorption Coefficient (cm^{-1})						
	H-3 (T)	**Pm-147**	**Ni-63**	**Sr-90**	**C-14**	**Zr-93**
ZnS:CuCl	9.02538	0.257048	1.61343	0.0718925	0.429347	1.61343
ZnS	20.7381	0.590633	3.70725	0.165191	0.986534	3.70725
ZnO	28.4249	0.809557	5.08138	0.226421	1.3522	5.08138
$Zn_2SiO_4:Mn^{2+}$	21.5494	0.613738	3.85228	0.171653	1.02513	3.85228
$SrAl_2O_4:Eu^{2+},Dy^{3+}$	18.0508	0.514096	3.22685	0.143785	0.858694	3.22685
$SrB_4O_7:Sm^{2+}$	20.3832	0.580524	3.6438	0.162364	0.969649	3.6438

The absorption coefficient is based on the maximum kinetic energies of the beta isotopes and density of the phosphors. In our results, we observed that absorption coefficient is inversely proportional to energy.

4.2.2 Reflection Coefficient

When a high-energy electron impinges upon a semiconductor, it undergoes two forms of scattering: elastic scattering and inelastic scattering. Elastic scattering, or electron backscattering, occurs at the surface of the semiconductor and can be thought of as electron "reflection" from the surface. No energy is transferred to the semiconductor lattice in this process. Only momentum is changed. These backscattered electrons are lost and cannot contribute to power generation in the crystal. The fraction of incident electrons that is backscattered is called the reflection coefficient (r), and is a strong function of the Z-number of the target crystal [22]:

$$r = -0.0254 + 0.016Z - 1.86x10^{-4}Z^2 + 8.3x10^{-7}Z^3 \qquad (4.3)$$

It can be seen that the smaller the target atom, the fewer the electrons that are backscattered. For a compound, reflection coefficient can be calculated from the relative weight fraction for each element.

Table 4.15 Calculated reflection coefficient values for some phosphorescent materials

Reflection Coefficient	
ZnS:CuCl	0.518607
ZnS	0.397813
ZnO	0.35956
$Zn_2SiO_4:Mn^{2+}$	0.482728
$SrAl_2O_4:Eu^{2+},Dy^{3+}$	0.66533
$SrB_4O_7:Sm^{2+}$	0.605171

The reflection coefficient values are calculated with Eqn. (4.3). Reflection coefficient is based on the atomic number of the phosphors. By using reflection and absorption coefficients finally generation rates for each phosphor are evaluated by using Eqn. (2.33) and are given in Table 4.16.

Table 4.16 The generation rate values based on the mean kinetic energies of the beta isotopes for phosphor mixtures.

Generation Rate (Bq/cm^3)						
	H-3 (T)	**Pm-147**	**Ni-63**	**Sr-90**	**C-14**	**Zr-93**
ZnS:CuCl	$8.543x10^{10}$	$2.627x10^{10}$	$4.206x10^{10}$	$2.331x10^{10}$	$3.522x10^{10}$	$5.283x10^{10}$
ZnS	$23.80x10^{10}$	$7.326x10^{10}$	$11.72x10^{10}$	$6.500x10^{10}$	$9.816x10^{10}$	$14.72x10^{10}$
ZnO	$37.71x10^{10}$	$11.60x10^{10}$	$18.58x10^{10}$	$10.29x10^{10}$	$15.54x10^{10}$	$23.32x10^{10}$
$Zn_2SiO_4:Mn^{2+}$	$14.70x10^{10}$	$4.521x10^{10}$	$7.244x10^{10}$	$4.014x10^{10}$	$6.060x10^{10}$	$9.090x10^{10}$
$SrAl_2O_4:Eu^{2+},Dy^{3+}$	$6.789x10^{10}$	$2.086x10^{10}$	$3.638x10^{10}$	$1.853x10^{10}$	$2.797x10^{10}$	$4.199x10^{10}$
$SrB_4O_7:Sm^{2+}$	$13.76x10^{10}$	$5.342x10^{10}$	$6.782x10^{10}$	$3.759x10^{10}$	$5.675x10^{10}$	$8.513x10^{10}$

The highest and lowest values for generation rate based on the energy beta source are found for ZnO, and $SrAl_2O_4:Eu^{2+},Dy^{3+}$ phosphor materials respectively.

CHAPTER 5
CONCLUSION

Radioluminescence nuclear batteries have undergone great development in recent decades. These phosphor-based nuclear battery systems have a wide range of applications, from long life power systems to aerospace systems. In addition, the phosphorus-based nuclear batteries offer a wide range of use advantages due to their rapid adaptation to nano-size and lightweight structures.

The phosphors absorb radiation from beta-derived nuclear cells. Therefore, the collision energy loss of the electrons is very important for determination of generation rate which gives the number of electron hole pairs in phosphors due to beta particles that are used for p-n or other types of junctions in betavoltaics. The relationship of the beta range and the phosphor layer thickness is the key to optimizing beta radioluminescence nuclear battery. The optimal phosphor layer must be of sufficient thickness to absorb most of beta particles and still allow for high-efficient transmission of the emitted luminescence.

In this study, we have analysed the stopping power, the range and the generation rate parameters of different phosphors containing Zn and Sr. Because radioluminescence spectrum of such phosphors is also visible region of electromagnetic spectrum that is suitable for betavoltaic energy conversion. Therefore, these phosphors are usually used in experimental studies for analysing the properties of beta radioluminescence nuclear battery [2,20].

Based on the beta source's energy values, mass stopping power values are calculated and given in Table 4.11. Mass stopping power parameters depend on mean excitation energy, atomic number, atomic mass, and the percent of the phosphors forming the mixture. From our results, it is observed that mass stopping power is inversely proportional to the energy values of beta source.

The range is important parameter for determining the thickness of phosphor material in the design of RL batteries. Density of phosphors and kinetic energy of the beta particles are important parameters for the beta range. At the same energy, the range is inversely proportional to the density of phosphors. From our results given in Table 4.12, it seen that if the kinetic energy of beta sources increases, the range also increases.

Electrical energy production efficiency for any design of indirect conversion battery build on the match of the spectral response curve of the PV cell is to the emission maximum of the luminescent material. The performance of batteries can be improved by balancing the rival effects of nuclear energy absorption and luminescence transmission. Therefore, the thickness of the phosphorus layer and the efficiency of RL transmission are critical for the design of the batteries. The beta particles in the phosphor layer is also an important factor to reduce energy conversion efficiency. Therefore, to increase the energy conversion efficiency of the battery, both high efficiency and transparent phosphorus should be selected. In addition, the activity and purity of the source should be increased.

It is well known that generation rate is the total number of electron-hole pairs produced by luminescence mechanism in phosphor materials. From Table 4.16, it is seen that number of electron hole pairs per unit volume for each phosphor compound is inversely proportional to the kinetic energy of beta source. This result can be explained as when beta particle enters into phosphor material suffers inelastic and elastic scattering. Due to these scattering mechanisms, beta particle loses its energy. Depending on these mechanisms, absorption coefficient of phosphor also decreases. These events cause to decrement in generation rate values for high beta energies.

Theoretical investigation of the properties of such phosphor compounds has not been studied in literature. This thesis will provide a basis for RL nuclear battery designers.

REFERENCES

[1] Nsimama, P. D., Ntwaeaborwa, O. M., Swart, H. C. (2011). The Effect of Different Gas Atmospheres on Luminescent Properties of Pulsed Laser Ablated SrAl2O4:Eu^{2+},Dy^{3+} Thin Films, *Journal of Luminescence*, **131(1)**, 119-125.

[2] Hong, L., Tang, X. B., Xu, Z. H., Liu, Y. P., Chen, D. (2014). Radioluminescent Nuclear Batteries with Different Phosphor Layers. *Nuclear Instruments and Methods in Physics Research Section B: Beam Interactions with Materials and Atoms*, **338**, 112-118.

[3] Tanuma, S., Powell, C. J., Penn, D. R. (2008). Calculations of Stopping Powers of 100 Ev–30 kev Electrons in 31 Elemental Solids. *Journal of Applied Physics*, **103**, 063707

[4] Syed, N. A. (2007). *Physics and Engineering of Radiation Detection Second Edition*, Elsevier USA.

[5] Bower, K. E., Barbanel, Y. A., Shreter, Y. G., Bohnert, G. W. (2002). *Polymers, Phosphors, and Voltaics for Radioisotope Microbatteries.* 109-201.

[6] Zhang, Z. R., Liu, Y. P., Tang, X. B., Xu, Z. H., Yuan, Z. C., Liu, K., Chen, W. (2018). GaAs Low-Energy X-ray Radioluminescence Nuclear Battery. *Nuclear Instruments and Methods in Physics Research Section B: Beam Interactions with Materials and Atoms,* **415,** 9-16.

[7] Russo, J., Litz, M., Ray, W. II, Rosen, G. M., Bigio, D. I., Fazio, R. (2017). Development of Tritiated Nitroxide for Nuclear Battery. *Applied Radiation and Isotopes,* **125**, 66-73.

[8] Jin, Z., Tang, X., Guo, X., Liu, Y., Xu, Z., Chen, W., Zhou, D. (2018). Design and Performance Study of Four Layer Radio-Voltaic and Dual-Effect Nuclear Batteries Based on γ-Ray, *Nuclear Instruments and Methods in Physics Research Section B: Beam Interactions with Materials and Atoms,* **428**, 47-55.

[9] Russo, J., Litz, M.., Ray, W., Smith, B., Moyers, R. (2017). A Radioluminescent Nuclear Battery Using Volumetric Configuration: 63Ni Solutions/ZnS:Cu, Al/InGaP. *Applied Radiation and Isotopes: Including Data, Instrumentation and Methods for Use in Agriculture, Industry and Medicine*, **130**, 66-74.

[10] Mark, A. Weaver, P. C. L., Watermann, M. L., Lukosi, E. D., Schott, R. J., Wisniewski, D. A. (2014). A Review of Nuclear Batteries. *Progress in Nuclear Energy,* **75**, 117-148.

[11] Kumar, V., Chaudhary, B., Sharma, V., Verma, K. (2019). *Radiation Effects in Polymeric Materials,* Springer Science and Business Media LLC.

[12] Turner, J. E. (2007). *Atoms, Radiation, and Radiation Protection Third Edition*, Wiley-VCH Verlag GmbH & Co. KGaA.

[13] Podgorsak, E. B. (2006). *"Radiation Physics for Medical Physicists",* Springer, Berlin, Heidelberg.

[14] Podgorsak, E. B. (2016). "*Radiation Physics for Medical Physicists 3rd Edition"*, Springer Science and Business Media LLC, Switzerland.

[15] An Introductory Chemistry Libretexts Textmap Organized Around Tro's Textbook Introductory Chemistry, Types of Radioactivity: Alfa, Beta and Gamma Decay, www. chem.libretexts.org.12.12.2018

[16] Nikjoo, H., Uehara, S., Emfietzoglou, D. (2012). *Interaction Of Radiation With Matter*, Boca Raton, London, New York.

[17] Andreeshchev, E. A., Kilin, S. F. (1978). Measurement of Absolute Radioluminescence Yield of Plastic Scintillator Excited by Co60 γ Rays, *Journal of Applied Spectroscopy*, **29(1)**, 799-803.

[18] Podgorsak, E. B. (2010). *Radiation Physics for Medical Physicists Second Edition*, Springer Nature, Springer-Verlag Berlin Heidelberg.

[19] Loveland, W., Morrissey, D. J., Seaborg, G. T. (2005). *Modern-Nuclear-Chemistry*, Wiley-Interscience.

[20] Xu, Z. H., Tang, X. B., Hong, L., Liu, Y. P., Chen, D. (2014). Development of a Beta Radioluminescence Nuclear Battery, *Nuclear Science and Techniques* **25(4),** 04063(1)-040603(6).

[21] Liu, Q C, Jia, B S, Wan, J. (1988). *Overview of Nuclear Science*. Harbin Institute of Technology Press.

[22] Olsen, L. C., (1972). Beta İrradiation of Silicon Junction Devices : Effects on Diffusion Length, *IEEE Transactions on Nuclear Science,* **19(6),** 375-381.

[23] Klein, C. A. (1968). Bandgap Dependence and Related Features of Radiation Ionization Energies in Semiconductors, *Journal of Applied Physics,* **39**, 2029-2038.

[24] Sachenko, A. V., Shkrebtii, A. I., Korkishko, R. M., Kostylyov, V. P., Kulish, M. R., Sokolovskyi, I. O. (2015). Efficiency Analysis of Betavoltaic Elements, *Solid-State Electronics*, **111**, 147-152.

[25] Penelope, A. R., Jerry, W. (2008). *Radiation physics*, Elsevier B.

[26] Murthy, K. V. R., Virk, H. S. (2013). Luminescence Phenomena: An Introduction, Defect and Diffusion Forum Trans Tech Publications, *Defect and Diffusion Forum,* **347,** 1-34.

[27] Shanker, V., Haranath, D., and Swati, G. (2015). Persistence Mechanisms and Applications of Long Afterglow Phosphors, *Defect and Diffusion Forum Trans Tech Publications*, **361,** 69-94.

[28] Kalyani, N. T., Hendrik, S., Dhoble. S. J. (2017). *Luminescence, Principles and Applications of Organic Light Emitting Diodes (OLEDs) 1st Edition*. Elsevier BV.

[29] Martin, B, and Ziegler, K. (1991). Cyclotrons and Their Applications. *Cyclotrons and their Applications: Twelfth International Conference,* Berlin, Germany.

[30] Bochev, B., Yordanov, G. (2014). Room Temperature Synthesis of Thioglycolate-Coated Zinc Sulfide (ZnS) Nanoparticles in Aqueous Medium and Their Physicochemical Characterization. *Colloids and Surfaces A: Physicochemical and Engineering Aspects*, **441**, 84-90.

[31] Sepyani, K., Afrand, M., Esfe, M. H. (2017). An Experimental Evaluation of The Effect of ZnO Nanoparticles on The Rheological Behavior of Engine Oil. *Journal of Molecular Liquids,* **236,** 198-204**.**

[32] Yürük, R. K., Tütüncüler, H. (2017). Investigation of The Effect of Beta Source and Phosphors on Photovoltaic Cells. *AIP Conference Proceedings*, **1815(1),** 040002(1)-040002(6).

[33] Chen, Z. G., Cheng, L., Zou, J. (2011). Growth and Optical Properties of Stocked Pyramid Zinc Sulfide Architectures. *CrystEngCom*, **13**, 5885-5890.

[34] Reynolds, D. C., Look, D. C., Jogai, B., (2001). Fine Structure on The Green Band in ZnO. *Journal of Applied Physics*, **89(11)**, 6189-6191.

[35] Zhang, J. M., Zhao, D. L., Shen, Z. M. (2010). Synthesis and Luminescent Properties of Mn^{2+}-Doped Zinc Silicate Phosphors by Sol-Gel Method. *Key Engineering Materials*, **434**, 214-216.

[36] Matsuzawa, T., Aoki, Y., Takeuchi, N., Murayama, Y. (1996). A New Long Phosphorescent Phosphor with High Brightness, $SrAl_2O_4:Eu^{2+},Dy^{3+}$. *The Electrochemical Society*, **143(8)**, 2670-2673.

[37] Yürük, R. K.**,** Tütüncüler, H. (2019). Theoretical Investigation of High-Efficiency GaN-Si Heterojunction Betavoltaic Battery, *Canadian Journal of Physics.*